Summer 2020

Microgel placement and plugging performance in sand filled fracture for conformance control

Baihua Lin

Department:

MICROGEL PLACEMENT AND PLUGGING PERFORMANCE IN SAND FILLED FRACTURE FOR CONFORMANCE CONTROL

by

BAIHUA LIN

A THESIS

Presented to the Graduate Faculty of the

MISSOURI UNIVERSITY OF SCIENCE AND TECHNOLOGY

In Partial Fulfillment of the Requirements for the Degree

MASTER OF SCIENCE IN PETROLEUM ENGINEERING

2020

Approved by:

Dr. Baojun Bai, Advisor
Dr. Ralph Flori
Dr. Mingzhen Wei

ABSTRACT

Preformed particle gels (PPG) has been widely applied for conformance control in heterogeneous reservoirs with fractures and super-K channels. As a plugging agent, PPG could plug the fractures or high permeability streaks and divert the displacing fluid into low permeability matrix. Many studies have been conducted to investigate the potential of PPGs as a water cut reduction and improved oil recovery agent using homogeneous sandpacks or heterogeneous core samples with man-made open fractures. However, no research has been carried out to understand how PPG injection and plugging performance will be changed if the fractures are filled with sands. Herein, the main objective of this work is to study the PPG plugging performance in a heterogeneous reservoir with a sand-filling fracture. To reach the objective, a core model with a sand-filling fracture was built to simulate the fractured reservoir. Three sizes of PPG with different swelling ratios were injected as a plugging agent. The gel migrations, pressure behaviors, oil recovery ratios and water cuts in different cases were recorded and analyzed. We found the gel injection pressure behaved as an up trending zigzag shape and was more sensitive to the gel swelling ratios than the particle sizes. Although the PPG plugging efficiency could be impaired by later chased polymer solution, the oil recovery showed an improvement of nearly 7% and a water cut reduction of 5% after gel treatment using the PPG with a larger swelling ratio. The gel migrations within the sand-filling fractures were observed by opening fractures after flooding tests. It showed that the gel with the lower swelling ratio did not play an effective role in plugging the pore spaces between sand grains, while the one with the higher swelling ratio had a positive effect on the plugging performance.

ACKNOWLEDGMENTS

First of all, I would like to express heartfelt gratefulness to my advisor, Dr. Baojun Bai, for his guidance and encouragement to my research. Every time I met the critical situation in my research, he always provides the way to solve the problem with his wisdom and patience. Under the careful cultivation of Dr. Bai in the three-research semesters, as a master student, I have already learnt how to face difficulties, developed the capability to think the solution of problems independently, and reinforced the capability of summarizing the research paper. In one word, so far, the all progresses I have made is by standing on the shoulders of Giants.

In addition, I would like to thank my committee members, Dr. Ralph Flori and Dr. Wei for their advice and patience.

Moreover, I wish to extend my thanks to United States Department of Energy (DOE), thanks for the financial support, without the help, it is impossible to complete the research. Furthermore, I would like to express my gratitude to my lab mates, Yandong Zhang and Yifu Long. Yandong Zhang supported me a lot in terms of revising the thesis with his excellent writing skills and giving moral support with his optimism. Yifu Long gave me the significant help in terms of setting up the experiment facilities and discussing the results with his rich experience. Thanks also go to my colleagues, Xindi Sun, Ze Wang, Shuda Zhao, Zhe Sun, HaifengDing, Shize Yin and Jiaming Geng for their help.

Finally, I would like to express my sincere gratitude to my parents, thanks for their encouragement and financial support.

TABLE OF CONTENTS

LIST OF ILLUSTRATIONS

Page

LIST OF TABLES

Page

NOMENCLATURE

Symbol	Description
BV	Bulk volume of the matrix
PV	Pore volume of the matrix
Φ	Porosity
Kab	Absolutely permeability of matrix
Swi	Initial water saturation in matrix
Soi	Initial oil saturation in matrix
OOIP	Original oil in place
RF	Oil recovery factor
WF	Water cut

1. INTRODUCTION

Heterogeneity is one of the most inevitable issues that petroleum engineers faces and requires to be solved during oil recovery processes. The reservoir heterogeneity often causes the channeling problem of injected water, which makes water bypass the un-swept zones/areas and thus leaves nearly two thirds of oil-in-place not to be recovered after primary and secondary recovery processes. Conformance issues widely exist in mature oilfields. Excessive water production caused by the conformance problems can cause a lot of industry concerns, such as shortening the well life, causing the corrosion, aggravating reservoir heterogeneity, and so on. Many enhanced oil recovery methods are available to improve the recovery of the remaining oil and control water production; however, these methods might not be efficient enough if the conformance issues are not solved.

Gel treatment has been successfully applied to solve reservoir conformance problems. Two typical types of polymer gels are often applied for it: in-situ gel and preformed gel. In-situ gel is formed in the reservoirs after gelation is placed in target location while preformed gel is formed before it is pumped into a reservoir. Due to the injection issue associate with preformed bulk gel, preformed particle gels (PPG) has drawn great interest for conformance control. Due to its advantages over in-situ gels, PPGs have been widely investigated and applied for conformance control in mature oilfields.

Extensive researches have been done to study the transport and plugging mechanisms of PPG through fractures using tube models made from steel tube,

transparent fracture model made from acrylic plates, open fracture models made from Berea sandstone, and sandpack models. However, no work has been carried out using fluid channeling models made from the composition of cores and sandpacked fractures.

A polymer flooding project is conducting in Alaska North Slope (ANS) which contains vast resources of heavy oils primarily concentrated in West Sak (also called Schrader Bluff) and Ugnu reservoirs. Early polymer breakthrough is a major concern for the success of a polymer flooding project because it will significantly reduce the efficiency of polymer flooding. This problem could be much worse for heavy oil reservoirs. Polymer gel treatments have often been applied in polymer flooding projects at the beginning, middle, or end of polymer injection to improve polymer injection conformance. Preformed particle gels have been widely applied to improve the conformance for water flooding and polymer flooding because they can preferentially enter super-K zones/streaks to reduce their permeability while minimizing the damage of gels on un-swept oil-rich zones (Imqam et. al., 2014, 2016, Bai et. al., 2007, 2013, Zhang and Bai, 2010, Bai et. al., 2008). It is of major importance to screen a proper particle gel that will be used to control the polymer flooding conformance and improve the utilization efficiency of the polymer project. The objective of this research is to build heterogeneous models and run experiments to know the extend to what microgel treatment can improve the conformance of polymer flooding in the reservoir.

2. LITERATURE REVIEW

2.1. AN INTRODUCTION OF GEL TREATMENT FOR ENHANCED OIL RECOVERY

Water channeling is one of the inevitable issues for petroleum engineer to solve in typically heterogenous reservoirs. Water channel will cause premature breakthrough and aggravate the heterogeneity in mature field by inducing severe factures. As a result, large quantities of oil will be remained in the unsweep zone or the lower permeability zone. Thus, water channeling issue will decrease the oil recovery and approach the reservoir economic limit earlier.

Gel treatment is the most mature and successful solution for solving the water channeling issue because of its mechanism that the gel particle will reduce the conductivity in the higher permeability fluid channel by plugging and reducing the permeability in this area. In-situ and preformed particle gel have been widely used for gel treatment. However, preformed particle gel has gradually replaced in-situ gel for gel treatment in recent years because preformed particle gel has overcome some problems of in-situ gel during the gel treatment process, for instance, uncontrol gelation time, shear degradation influence and dilution by formation water (Bai et al., 2007).

2.2. GEL TREATMENT TYPES

2.2.1. In-situ Polymer Gel Treatment. As reviewed by Bai et al (2015), the in-situ polymer gel displayed a 3D network and liquid behavior. The gel is constituted by high molecular weight polymers connected by a kind of crosslinking agent, and there are two types of crosslinking systems, which are metallic and organic crosslinked

systems(Bai et al., 2015) .In the 1970s, Needham from Philips Co as a forerunner to synthesize the first in-situ gels by using partially hydrolyzed polyacrylamides and aluminum citrate (Needham et al., 1974). Thereafter, the in-situ gel with polyacrylamide as the primary gel system has been widespread for enhanced oil recovery.

Metallic cross-linked PAM system: In the metallic cross-linked PAM system, the multivalent metal ions such as Zr(IV), Al(III), Cr(III) are the cross-linkers, which will react with carboxyl group of polyacrylamide when being added to an HPAM solution. In the 1970s, aluminum sulfate was typically used to synthesize cross-linked HPAM. However, some gel treatment issues has appeared in the filed applications. First, due to synthesizing with aluminum sulfate, the gel was so sensitive that it was hard to control the gelation time when injecting into the formation with higher pH value. Second, the gelation time will be abbreviated when injecting into the reservoir with higher temperature. Third, in 1981, Ecological analysts Inc. reported the Cr (VI) is carcinogenic (Ecological analysts Inc. 1981). The above problems had been solved in 1984, Sydansk et al. synthesized a new polymer gel system by using HPAM/chromium (III) acetate (Sydansk et al 1988). The application results of acrylamide-polymer/chromium (III) carboxylate gels have been reported by Southwell et al. in 1994, the additional increment of oil recovery is 1,200,000 stock tank barrels (Southwell et al. 1994). Some researchers also did some studies about injection properties of in-situ gel with metallic cross-linked PAM system. The research direction is based on the polymer and cross-linker solution retention on the pore surfaces during the in-situ gel injection. Mack and Smith evaluated the in-depth dispersion of in-situ gel with HPAM/aluminum citrate, a dispersed gel state has been introduced, the colloidal dispersion gel (CDG). A CDG can

be determined when a gelatinous substance accumulates on the exit side of a screen viscometer. Mack et al. claimed that colloidal dispersion gels could move through the sand face without plugging and travel a significant distance into the reservoir (Mack and Smith et al. 1994). However, some laboratory tests have shown that CDG can only penetrate into extremely high permeability zones and can propagate in depth in laboratory sand packs with a permeability of several Darcies (Al-Assi et al,.2006. Green D W et al. 1995. Seright R et al. 2007).

Organic cross-linked PAM systems: To apply the in-situ gel under a harsh reservoir condition, Chang et al. synthesized an organically cross-linked gel, which the cross-linking reacts between phenolic compounds and formaldehyde (Chang P et al. 1984). The gel system is named as Flowperm325. Some researches confirmed that the gelation occurs at the pH over 9 and doesn't occur at the pH below 5. Moreover, the temperature limit is 149 °C (Seright F et al. 1991. Zhuang Y et al. 2000 and Hutchins R et al. 1996.). To obtain longer gel delays, Hutchins et al. combined hydroquinone (HQ) and hexamethylenetetramine (HMTA) as cross-linked system to synthesize a cross-linked gel which was applied under 176.7°C condition and kept stable about 5 months. Doven et al. used HQ as the second cross-linkers to stabilize the gel with HTMA cross-linkers, and the results found the gel performance was stable under 176.7°C by combining two cross-linkers but the cost is higher so that no report is available about whether it has been applied in oil fields. Until 1997, a unique organic cross-linked PAM system had been described by Morgan et al, which was relied on an acrylamide/ t-butyl acrylate copolymer (PAtBA) cross-linked with polyethyleneimine (PEI) instead of the HQ and HMTA combination. And the gel propagation and thermal stability were verified by Hardy et al

in 1998, since then, the gel with organic cross-linked PAM systems has been widely prevalent in oil field.

2.2.2. Preformed Particle Gel Treatment. As reviewed by Bai et al (2015), preformed particle gel is a kind of superabsorbent polymers (SAP). SAPs are three-dimensional networks of cross-linked polymer chains, which can absorb more than several to hundreds of times their mass of water due to the capillarity and osmosis. The crosslinker concentration affects the gel swelling ratio. Slightly cross-linked polymer can absorb more water but the gel strength is weaker in the normal (Bai et al., 2015). The preformed particle gel system can be classified by different gel sizes and the applications limited to reservoirs, which includes millimeter-sized (Coste et al 2000, Bai et al 2007), micrometer-sized (Chauveteau et al 1999, 2001; Rousseau et al 2005; Zaitoun et al. 2007) and submicro-sized preformed particle gels (Pritchett et al 2003, Frampton et al 2004).

Millimeter-sized Preformed particle gels. The preformed particle gels were synthesized by acrylamide and N,N'-methylenebisacrylamide which are used as monomer and cross-linker separately. The dry preformed particle gels were prepared with solution polymerization method and followed the application limited to reservoirs (fractures or fracture-like channels) to crush and sieve gel size to millimeter level. The dry preformed particle gels will be prepared to form gel particle dispersion by absorbing aqueous solutions before pumping into a well (Bai et al. 2013). Abedi Lenji et al (2018) did a comprehensive study about superabsorbent PPGs that the swelling ratio of weight is around 1000 to 2000 times. The study stated that by increasing the concentration of polymer, crosslinker and salinity to swell the gel particle, the PPG swelling ratio will decrease dramatically but the gel strength will increase. However, the swelling ratio

increased to highest value under the pH level from five to nine and no obvious change when the temperature increased to 100 °C (Abedi Lenji et al. 2018). During the gel injection process, one of the studies of gel dehydration was done by Song et al (2018). They found the dehydration decreased with increased gel injection rate, fracture width, and brine concentration in the open fracture and the definition of gel pack has been mentioned (Song et al. 2018).

The oil filed application of Millimeter-sized Preformed particle gels began in 1999 in China for conformance control, so far they have been applied in more than 10,000 wells for reducing water and polymer production in water flooding aeras (Bai et al, 2008. Liu et al, 2006.). The application of PPG for CO2 breakthrough control has also been processed by Kinder-Morgan, Halliburton, and Occidental in CO2 flooding areas (Larkin et al, 2008.).

Some researches about the millimeter-sized preformed particle gel transportation behaviors, factors affecting gel performance and gel application combined with other methods were comprehensively investigated by different researchers in recent 20 years. For the gel transportation behaviors studies, Coste et al. in 2000 used a glass micro model to simulate the gel propagation in the large pore throat, and three transportation behaviors have been discovered, which included particle deformation, particle shrinking by the expulsion of water, and particle breakage (Coste et al. 2000). In 2007, Bai et al used the same methods above to investigate more profoundly, in which six propagating patterns in Figure 2.1 were shown which included direct passing, adsorption and retention, deformation and passing, snap-off and passing, shrinking and passing, and trapping (Bai et al. 2007).

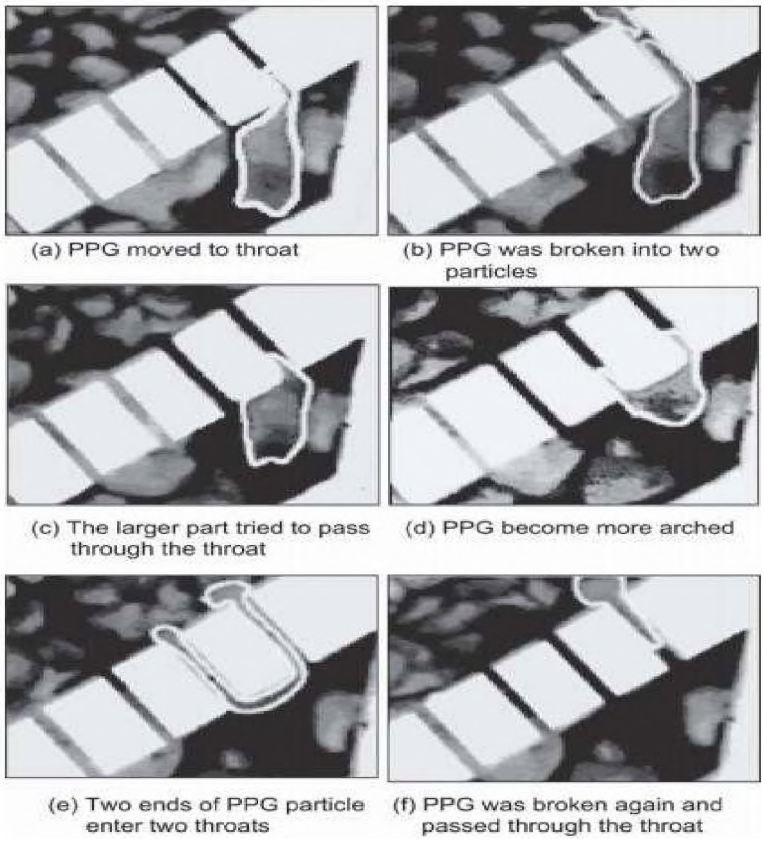

Figure 2.1 A process of a particle transporting through throats at the simplified (Bai et al. 2007).

Moreover, Zhang et al. concluded that the PPG performed a piton-like behavior during injection through open fractures (Zhang et al. 2010). Without the study of PPG through the constant width of throat and fractures, Imqam et al. did a study of PPG through the open conduits with varying internal diameters, and the study reported that the gel particle size can be reduced due to gel dehydration and breakdown (Imqam et al. 2015). In addition, Imqam et al. continued his study to investigate more profoundly by using similar experimental setup, and he concluded two transport mechanisms of PPG through nonuniform conduits, 1) In the choke point, PPG will pass, accumulation and break. 2) The choke size, conduit length and diameter ratio of particle size and conduit

size will influence the gel dehydration and breakdown during gel injection process. (Imqam et al.2017). Elsharafi et al. (2012) also studied the preformed particle gel propagation behavior on unswept areas, the study reported that millimeter-sized PPG will not pass through the unswept area of which permeability is below 320 mD and a permeable gel cake has been formed on the inlet surface of low- permeability cores.

The other research area is about factors impacting gel performance, which includes PPG injection pressure, resistance factor and formation damage. Zhang et al. (2010) concluded that the injection pressure and the resistance factor increase with higher brine concentration during the PPG through the open fractures. Moreover, Zhang et al (2010) also proposed the fracture width is another factor to affect injection pressure, and this proposal was confirmed by Imqam et al (2017) and Sun et al (2019). Imqam et al injected PPG through heterogeneous void-space conduits and concluded that the injection pressure increases when the width of fracture decreases (Imqam et al. 2017). Sun et al. found that comparing to the open fracture filled with larger calcite particles in the fracture, a higher breakthrough pressure was met when PPG was injected into the smaller diameter of conduit (Sun et al. 2019). Imqam et al. (2017) also evaluate the effect of the particle/opening ratio to the gel-threshold pressure and the stable injection pressure, the results demonstrate both pressures are in direct proportion to the ratio. Moreover, Fakher (2017) generated three mathematical models to predict the resistance factor and injection pressure to PPG injectivity by adopting the experiment setup of Zhang et al. (2010) and Imqam et al. (2017). In addition, Sun et al. reported the gel strength is another factor to influence the injection pressure and the resistance factor when PPG combined low salinity waterflooding in the fractured reservoirs (Sun et al. 2018). The formation damage

of PPG is defined as the small portion of gel particle penetrate into unswept zone and form a filter cake at the surface of unsweep zone during the gel flooding process. The formation damage is often found around the wellbore area which can significantly reduce the permeability around the wellbore and take a negative effect of later displacement flooding processes. Elsharafi and Bai et al. used a filtration apparatus to illustrate above formation damage which was shown in Figure 2.2 and find out the formation damage can be mitigated by controlling the particle size and the brine concentration (Elsharafi and Bai et al. 2012).And the chemical method by using hydrochloric acid (HCL) as breaker is another effective solution to mitigate the PPG formation damage (Imqam et al. 2014). Furthermore, Wang et al. evaluate few oxidizing breakers for mitigating formation damage, and the results demonstrated the breaker which by using NaOH to activate Na2S2O8 was most effective (Wang et al. 2019).

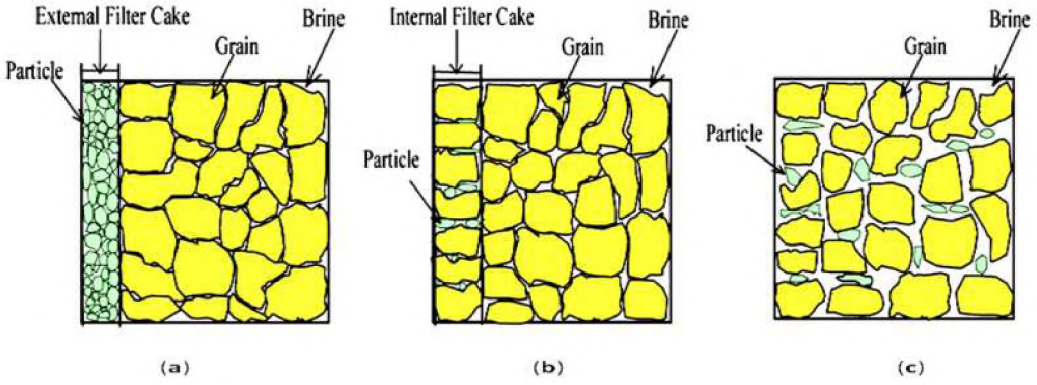

Figure 2.2 Schematic of PPG formation damage: a) external filter cake. b) internal filter cake. c) particle penetration (Elsharafi And Bai Et Al. 2012).

To improve the gel plugging and placement performance, some researchers did some studies by processing gel treatment to combine with other methods. Muchammed et

al (2014) investigated combining PPG treatment and surfactant methods for improving oil recovery in oil-wet fractured reservoir. By analyzing the results of injecting PPG and surfactant mixture and sequentially injecting two solutions, Muchammed et al reported that the coupled method accelerated the oil recovery and led to a higher injection pressure gradient (Muchammed et al. 2014). Moreover, Sun et al. (2018) studied the gel treatment by combining low salinity waterflooding to improve the conformance in fractures, and she concluded that the final oil recovery ratio is the highest comparing to that applying individually.

Microgels. In 2001, Chauveteau et al. found that the micrometer-sized particle gel plugged in the pore throat during in-situ HPAM/zirconium (IV) injection, and he explained it as a new crosslinking between the macromolecules (Chauveteau et al. 2001). This proposal was confirmed by Rousseau et al, they found that the polymers with a high degree of sulfonations tend to adsorbed around the pore surface (Rousseau et al.2005). Following the above proposal and confirmation, Chauveteau et al decided to apply microgel instead of in-situ gel, the micron gel they synthesized was using a terpolymer of acrylamide containing 2% acrylates and 2% sulfonated groups as monomer, and zirconium (IV) lactate as cross-linker, and the gel size can be determined by gel rupture process. Nearly ten gas storage reservoirs had been applied the above microgel treatment system which was reported by Zaitoun et al (Zaitoun et al. 2007). The typical microgel size is about 1-3 μm (Chauvereau et al. 2001). Table 2.1 lists the lab works with different gel particle size and application models (Dupuis et al., 2016, Goudarzi et al., 2014, Ali K et al., 2018, Chuan-jin et al., 2012, Guanglun et al., 2012, Imqam et al., 2015, Wu et al., 2013).

Table 2.1 The previous lab works of microgel with different size.

Authors	Gel size (μm)	Objectives	Conclusions
Dupuis et al, 2016	2	Test the different small microgel (SMG) concentration performance in sandstone core with residual oil	As the microgel concentration increases, the resistance factor and residual resistance factor increase.
Lei et al. and Yao et al, 2012	10-60	Study the factors which affect the elastic microspheres plugging performance in sand pack.	The contrast ratio between sphere and porous media is a significant factor to affect the residual resistance factor.
Imqam et al, 2015	70-90	Evaluate the microgel performance in non-crossflow heterogeneous model through the two different permeability parallel non-crossflow sand packs, which the setup was illustrated in Figure 2.3.	The microgel plugging performance better in the reservoir with more heterogenous properties.
Goudarzi et al, 2014	100-200	Understand the microgel propagation behavior by injecting microgel into Berea sandstone core and developed a numerical reservoir simulator to optimize the gel treatment results.	The mechanism of microgel transport in Figure 2.4 was been explained and a numerical reservoir simulator was developed. The core flooding results was successfully marched shown in Figure 2.5.
Wu et al, 2013	100-800	Establish the relationship between microgel size and reservoir permeability heterogeneity through the two heterogeneous parallel non-crossflow sand packs.	the excessive small size gel will not block the high permeability area well enough and will be migrated out during subsequent water injection
Ali K et al, 2018	250 and 850	Evaluate the microgel and low salinity waterflooding combining methods performance in non-crossflow heterogeneous reservoir through the two parallel non-crossflow sandstone cores.	Compare with sequent injecting two agents, the performance of PPG microgel is better when the gel is swelled in a low salinity concentration brine then injected together.

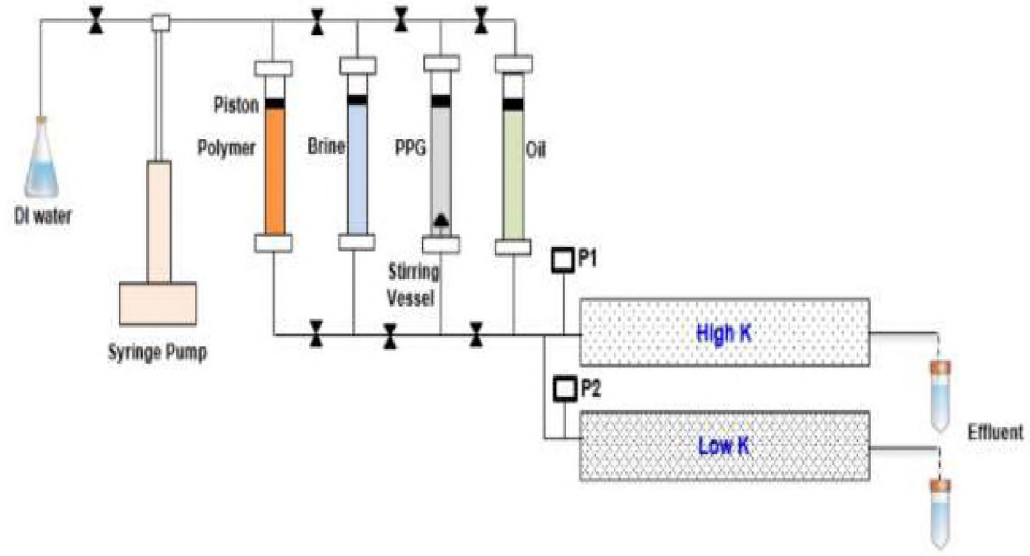

Figure 2.3 Experiments setup of non-crossflow heterogeneous model (Imqam et al, 2015).

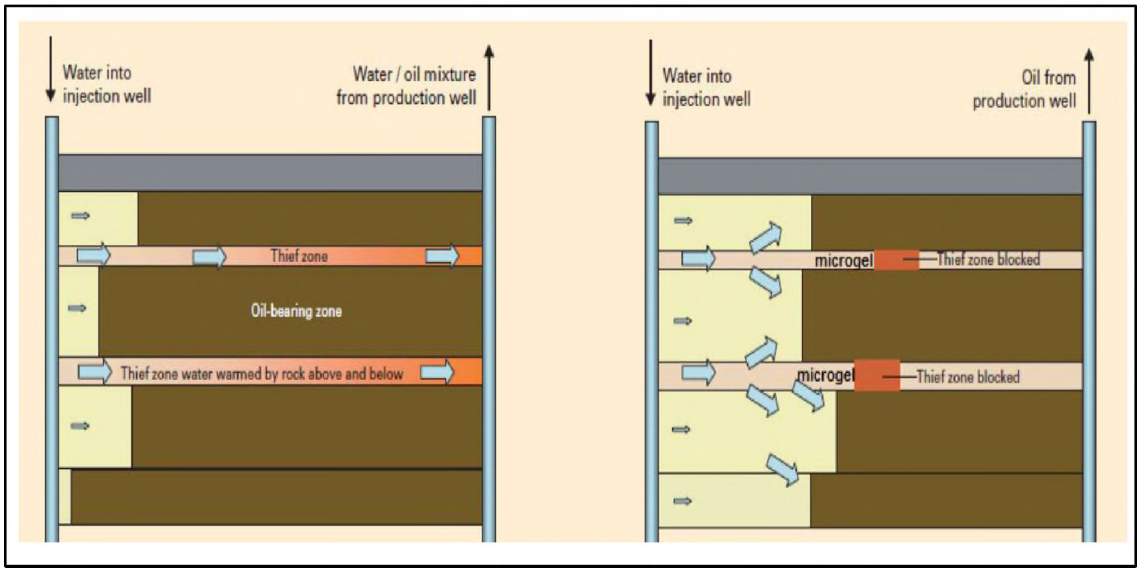

Figure 2.4 The mechanism of microgel transport on the rock surface in thief zones (Goudarzi Et Al, 2012).

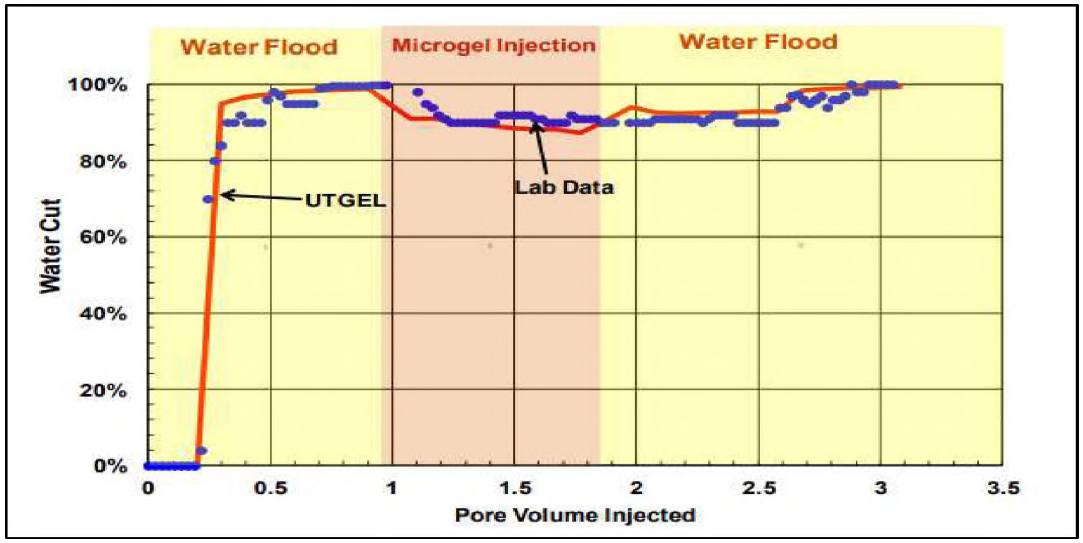

Figure 2.5 Comparison of history results (blue circles) and simulated results (red curve) water cut for berea coreflood (Goudarzi et al, 2012).

Submicron-sized particle gels (Bright Water^{TM}). A submicron-sized particle gel system has been proposed by both Pritchett et al. (Pritchett et al., 2003) and Frampton et al. (Frampton et al., 2004) for conformance control problems. The application of this particle gel is injected to block the thief zone with a several-hundred-millidarcy permeability; thus, the displacing fluid can be diverted to lower permeability zone in the in-depth of a reservoir. The key feature of this submicron-sized particle gels system is the microgels with a thermo-responsive property. As the underground temperature increases, the labile cross- linker in the gel network begins to de-crosslink, and thus the surface area of gel particle increases and absorbs more surrounding fluids.

3. EFFECT OF MICROGEL PLACEMENT AND PLUGGING PERFORMANCE IN SAND FILLED FRACTURE

3.1. EXPERIMENTAL MATERIALS

Microgel. For this study, two types of commercial preformed particle gel with different swelling ratios of 15 and 60 times were used. The swelling ratio tests are shown in Figure 3.1 Both kinds of particle gels, which synthesized by acrylamide, polyacrylamide copolymer and acrylic acid, are commercial superabsorbent polymers. During the whole experiment process, three different dry particle sizes (<62 μm, 62-88 μm, >88 μm) were chosen for each kind of gel. The Table 3.1 has already illustrated the gel size and type selections for different six experiments.

Table 3.1 The gel swelling ratio and size for each experiment.

No. Exp	Gel swelling ratio	Gel size
DE-1	15	120-230 mesh
DE-2	15	120-230 mesh
MPA-1	15	120-230 mesh
MPA-2	15	170-230 mesh
MPC-0	60	<230 mesh
MPC-1	60	<230 mesh
MPC-2	60	170-230 mesh

Polymer. A commercial polyacrylamide- based polymer (3630) was used to prepare a 1300 ppm polymer solution with the low salinity water, which has degree of hydrolysis of around 25% to 30%, molecular weight of 20 million Dalton and viscosity of 45 cp.

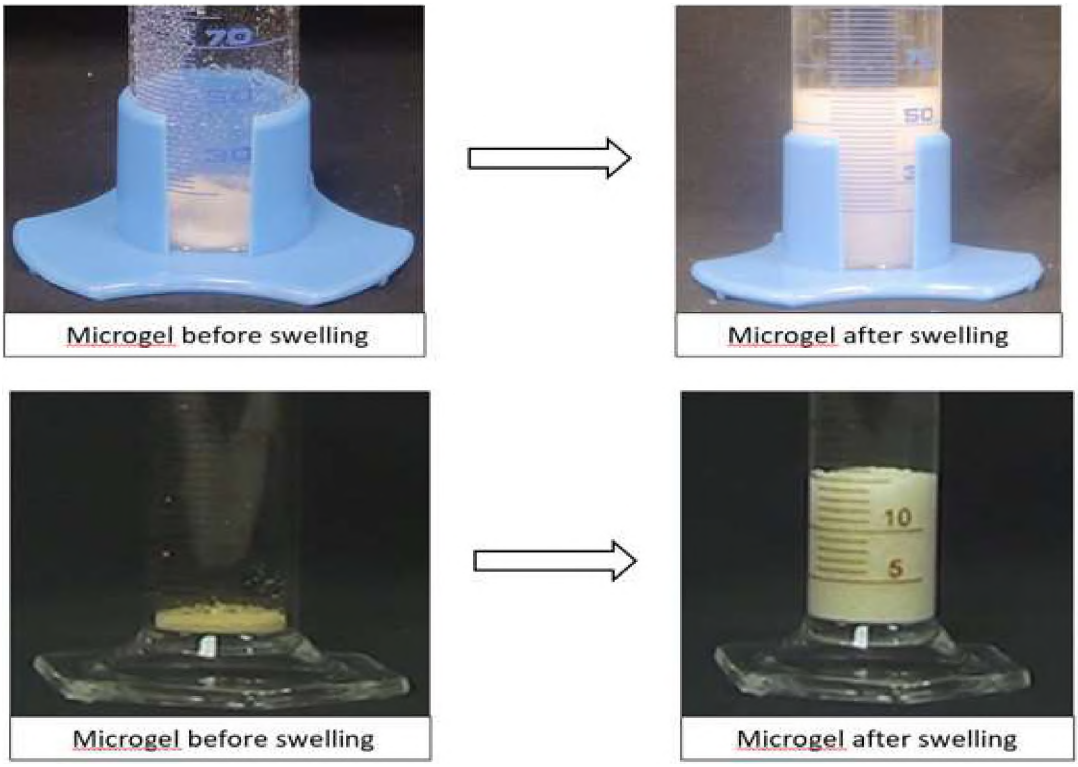

Figure 3.1 Swelling test of microgels with different swelling ratios (upper) 60 times (below) 15 times.

Oil. A heavy oil which is provided by Alaska reservoir, and the viscosity is 202 c.p, and the API gravity is 19° at 71°F which is provided by Hilcorp LLC.

Brine. Sodium chloride (NaCl) was used to prepare brines of two concentrations for the experiments. One is the low salinity water with the brine concentration of around

2500 ppm, the other one is the normal salinity water with the brine concentration of around 27500 ppm referred to the injected brine salinity and the formation water salinity in Alaska oil field. The compositions of these two brines are demonstrated and shown detail in Table 3.2.

Table 3.2 Composition of the normal and low salinity water.

Name	Description	Density (g/ml)	Salinity (ppm)	Composition (ppm)
Synthetic formation brine	SFB (normal salinity water)	1.062	27500	Na^+ : 10086.0 K+: 80.2 Ca2+: 218.5 Mg2+: 281.6 Cl-: 16834.4
Synthetic injection brine	SIB (Low salinity water)	1.03	2498	Na^+ : 859.5 K+: 4.1 Ca2+: 97.9 Mg2+: 8.7 Cl-: 1527.6

Sand. Two types of Silica sand were used in all experiments. For the first four experiments, the sand provided by Alaska oil field was used and the grain size distribution is in Figure 3.2. For the last three experiments, commercial sand with the grain size of between 30 to 40 mesh was used.

3.2. CORE PREPARATION AND EXPERIMENTAL MODEL DESCRIPTION

Core. Seven core samples were used in experiments. All core samples were cylindrically drilled from sandstone cubic rocks, then the fractures were created by sawing the cores into two half- cylindrical cores lengthwise following the centerline.

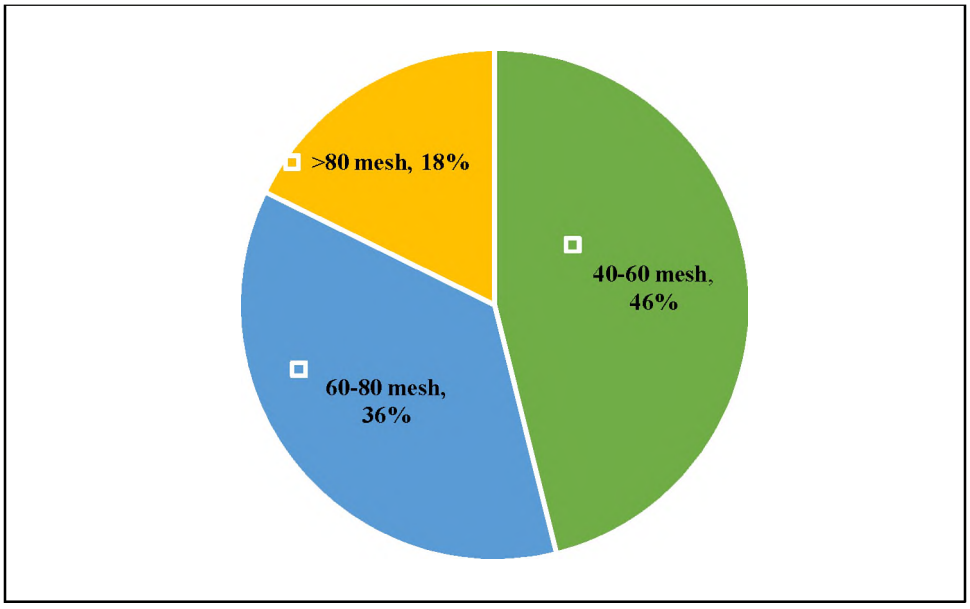

Figure 3.2 Alaska sand size distribution.

Figure 3.3 demonstrates the original sandstone cubic rocks and the fracture creation process and the dimensions and properties of each core samples Table 3.3 lists.

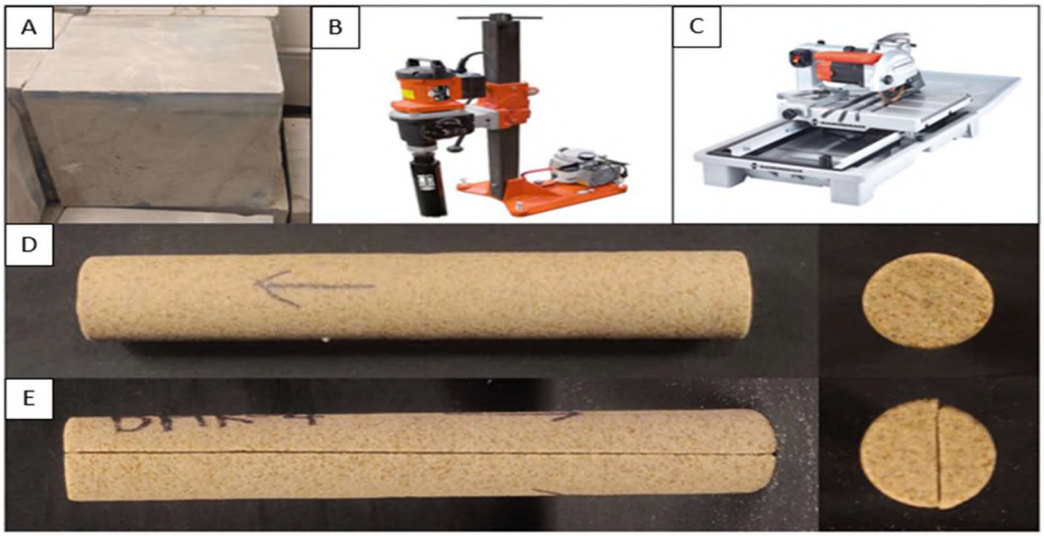

Figure 3.3 The cubic stone and related machines for creating the fracture. a) cubic sandstone. b) the core drill rig. c) the wet tile saw. d) the core sample after drilling. e) the core sample after sawing.

Table 3.3 Core samples dimensions and properties before and after fractured.

Core ID	Initial core dimensions and properties before fractured								Core properties after fracture		
	L, cm	d, cm	BV, cm3	PV, cm3	Φ, %	Kabs, md	Swi, %	Soi, %	BV, cm3	PV, cm3	OOIP, cm3
DE-1	15.05	2.51	74.47	19.54	26.2%	95	32%	68%	67.72	17.74	12.06
DE-2	13.69	2.51	67.25	15.15	23%	497	32%	68%	61.11	13.77	9.40
MPA 1	14.7	2.51	72.74	17.07	23.5%	506	34%	66%	63.45	14.89	9.16
MPA 2	14.7	2.51	72.74	17.07	23.4%	506	34%	66%	63.45	14.88	9.15
MPC 0	15	2.51	73.69	16.01	22%	518	100%	0%	61.23	13.22	0
MPC 1	15	2.51	73.69	16.01	22%	517	30%	70%	61.79	13.42	9.24
MPC 2	15	2.51	73.69	15.90	22%	520	32%	68%	60.64	13.08	8.89

Experimental model. Figure 3.4 provided the sketches of the experimental 'sandwich' model. The cylindrical core sample was first drilled from the cubic sandstone rock and then saturated with the Alaska heavy oil as shown in Figure 3.5. After being cut from the middle, two thin steel belts will be supporting the fracture and the thickness of belts will be specified in the later table. The sand was then filled into the fracture and compacted tight before sealing the two semi-cylindrical cores using Epoxy. Finally, enwinding the Teflon to compact the model tightly enough, and the final views of model was shown in bottom photos of Figure 3.5.

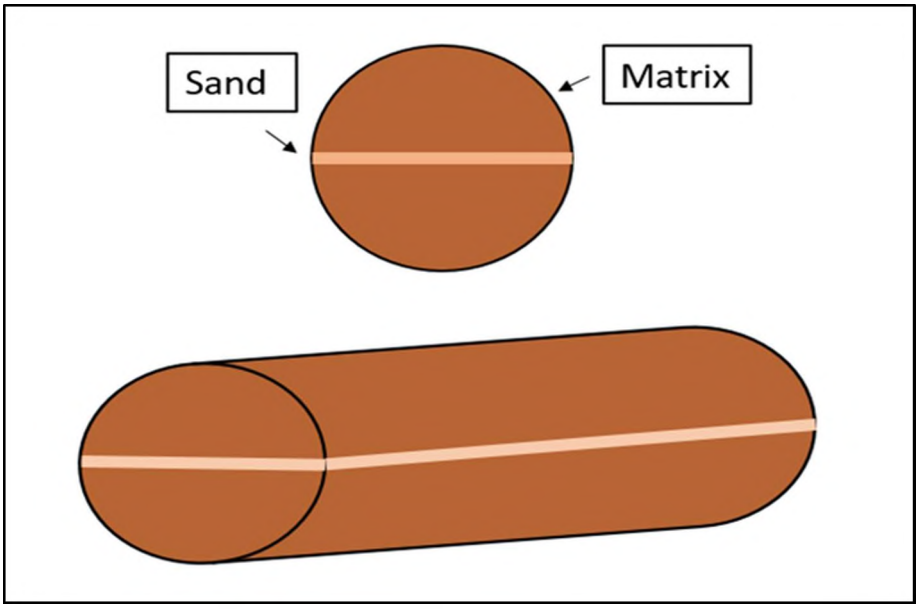

Figure 3.4 Experimental model sketches.

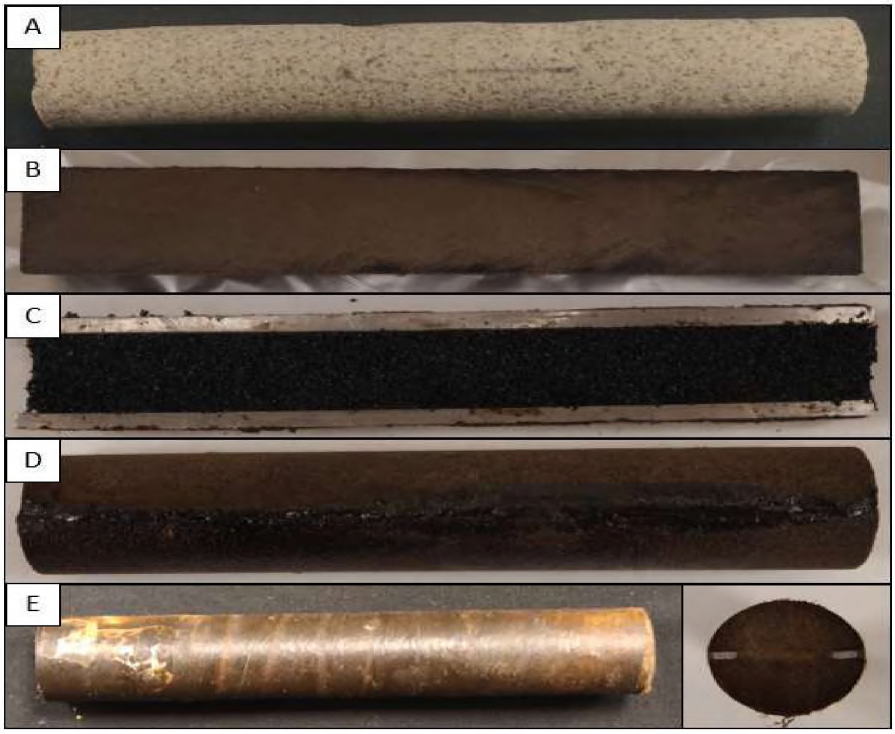

Figure 3.5 The preparations of experiment model. a) core sample before cut. b) saturate and cut the core sample. c) create open fracture and fill the sand. d) glue the fracture with epoxy. e) pack the core sample with Teflon.

3.3. EXPERIMENTAL SETUP AND PROCEDURES

Sand filled fracture Heterogeneity Apparatus Description. A sand filled fracture model was designed to simulate the true and complex reservoir condition which is heterogeneous. Figure 3.6 illustrates the sand filled fracture apparatus used to process the experiments. A heterogeneous sand filled fracture model was designed to study the microgel placement and plugging performance in the reservoir with obvious heterogeneous difference.

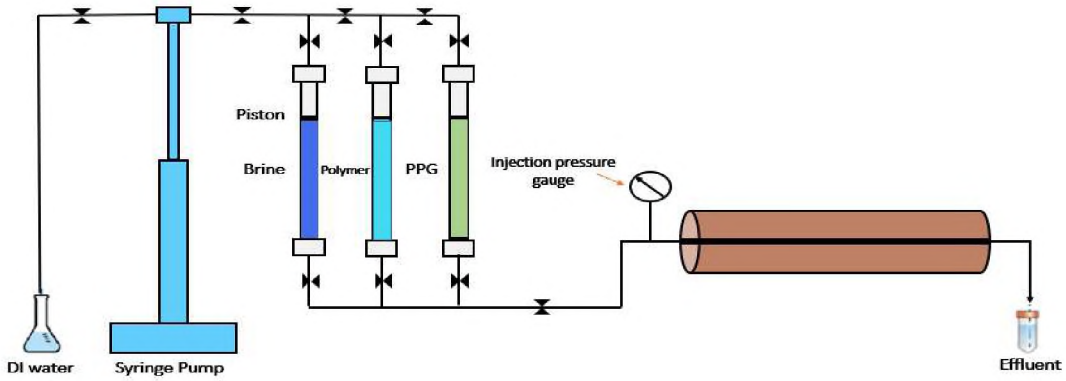

Figure 3.6 Schematic diagram of the experimental apparatus.

Experiment mechanism. As shown in the Figure 3.7, Due to the fluid channeling effect, the early breakthrough will happen and nearly no any oil which was saturated in the matrix will be displaced. Then, the gel particle will be injected and retained in the channels to plug and reduce the permeability in fluid channel. After gel injection, the conductivity in fluid channel has been reduced, the displacement fluid into matrix area, which makes micro-gel play a role to perform the conformance control.

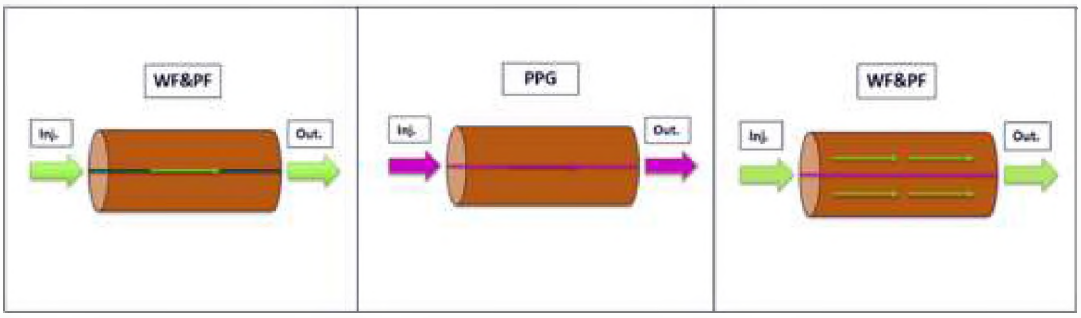

Figure 3.7 The mechanism of the gel treatment.

Experimental procedure. Without the experiment MPC-0, there are five procedures in other five experiments, the basic procedures were specified as follow and the injection volume of all procedures in each experiment are shown in Table 3.4.

Initial low salinity water Preflush. The low salinity water which was mentioned in material section will be injected into the inlet of sand filled fracture with the flow rate is 0.1 ml/min, the total injection volume was calculated when nearly no more oil was produced, but each experiments is different, which will be specified in Table 3.4. The objective of this waterflooding is to simulate the real oil recovery process in the reservoir. Collecting the oil drops from the effluent to calculate the water cut and oil recovery ratio and recording the injection pressure during the waterflooding process to calculate the water residual resistance factor.

First polymer flooding process. The 0.4 pore volume polymer solution will be injected with the flow rate is 0.1 ml/min. The objective of the polymer flooding is not only simulating the real oil recovery process in reservoir, but it also expends the potential energy of oil recovery in the model to help to evaluate the gel performance. Collecting the oil drops from the effluent to calculate the water cut and oil recovery ratio.

Microgel placement. The dry gel particle was swelled in the low salinity water, and the concentrations of swelling gel mixture are 1%. Then left about 5 hours to fully swell. After finish gel particle swelling process, put the swelled gel mixture into an automatic stirring accumulator, the syringe pump will push the piston to inject the gel particle into the experimental model. The flow rate is 0.1 ml/min and the other gel injection parameters like the size, type and volume will be listed in Table 3.4. Collecting the oil drops from the effluent to calculate the water cut and oil recovery ratio and recording the injection pressure during the gel flooding process. After finishing the gel flooding the process, cleaning the pipes near the injection area to avoid following fluid will be blocked due to the gel particle was remained in the pipes.

Second polymer flooding process. The injection volume is different in each experiment which was demonstrated in Table 3.4, but the flow rater is continue 0.1 ml/min. The objective of this flooding process is to evaluate the gel plugging efficiency by recording the injection pressure and comparing the water cut in fist polymer flooding process.

Second low salinity water flooding. Still injecting the same concentration salinity water with the 0.1 ml/min injection rate, and stopping to inject the salinity water when there is no more oil produced and the pressure reach a plateau.

3.4. EXPERIMENT RESULTS

The seven individual experiments were investigated the extent to study what microgel treatment can improve the conformance of polymer flooding in heavy oil using heterogenous models with channels. Three mainly orientations to analysis the results and

Table 3.4 The injection parameter of each procedures in different experiments.

No. Exp	Total injection volume of 1st water flooding	Total injection volume of 1st polymer flooding	Total injection volume of gel flooding process	Total injection volume of 2nd polymer flooding
DE-1	7.8PV	0.4 PV	1.1 PV	0.4 PV
DE-2	0.4PV	0.4 PV	2.35 PV	0.4 PV
MPA-1	0.6PV	0.4 PV	0.4 PV	0.4 PV
MPA-2	0.6PV	0.4 PV	0.6 PV	0.4 PV
MPC-0	---	---	---	---
MPC-1	0.6PV	0.4 PV	4.6 PV	3.6 PV
MPC-2	0.6PV	0.4 PV	4.5 PV	3.6 PV

achieve the objective mentioned above. First of all, with two demonstrative experiments to setup a feasible heterogeneous model with fluid channel, and the information of each experimental models has been listed in Table 3.5.

Then a preliminary study will be proceeded to determine the feasible injection parameters to be used for future study. Finally, the last three experiments were study the effect of microgel treatment on the conformance control efficiency of polymer flooding. The Table 3.6 shown the distribution and objectives of each experiments.

3.4.1. The Results of First Demonstrative Experiment. The below content covered the results and modification of the first demonstrative experiment.

3.4.1.1. First demonstrative experiment of microgel performance in sand filled fracture results (DE-1). The following results discussed the microgel placement and plugging performance in sand filled fracture, which includes water cut and oil recovery ratio change, pressure behavior, and gel migration.

Table 3.5 The information of each experimental models.

No. Exp	The height of fracture (mm)	Sand size (mesh)	Bulk volume (cm^3)	Pore volume (cm^3)	porosity	Soi	Swi	OOIP (cm^3)
DE-1	1.00	40-60	70.60	19.90	0.28	0.71	0.29	14.22
DE-2	1.00	40-60	63.72	15.73	0.25	0.72	0.28	11.36
MPA-1	1.00	40-60	66.26	17.00	0.26	0.66	0.34	11.27
MPA-2	1.00	40-60	66.23	16.99	0.26	0.66	0.34	11.25
MPC-0	1.50	30-40	61.23	13.22	0.22	---	---	---
MPC-1	1.50	30-40	65.77	15.56	0.24	0.73	0.27	11.39
MPC-2	1.50	30-40	64.57	15.22	0.24	0.72	0.28	11.03

The results of water cut, oil recovery ratio, and pressure behavior. As Figure 3.8 illustrated, in the first water flooding process, which included 4.7 PV high salinity and 2.6 PV low salinity water flooding. The oil recovery ratio is 7.3% at the end of the water flooding process. Compared the RF results in these two different salinity water flooding

Table 3.6 The distribution and objectives of each experiments.

No. Exp	Description	Objective
DE-1	The first demonstrative experiment of microgel performance in sand filled fracture.	Establish feasibility of the experimental model and experimental procedures.
DE-2	The second demonstrative experiment of microgel performance in sand filled fracture.	
MPA-1	The first experiment of microgel application in Alaska sand filled fracture.	Optimize the gel treatment and find out the feasible gel treatment scheme.
MPA-2	The second experiment of microgel application in Alaska sand filled fracture.	
MPC-0	The experiment of microgel application in commercial sand filled fracture without oil recovery process.	Investigate the gel placement and plugging performance for conformance control
MPC-1	The first experiment of microgel application in commercial sand filled fracture.	
MPC-2	The second experiment of microgel application in commercial sand filled fracture.	

processes, the increment of RF is 4.3% in low salinity water flooding, which is 1.4% higher than the increment in high salinity water flooding. The reason why lower salinity water is more contributing in terms of oil displacement efficiency is that the lower salinity water alters the rock wettability from oil-wet to water-wet (Zhang P et al. 2007). The improvement of oil recovery can be elucidated in the water cut curve of Figure 3.8. As the first 0.3 PV low salinity water being injected, the wettability changed rapidly so that the water cut sharply decreased to 86% simultaneously. After different salinity water injections, 0.4 PV of polymer solution was injected. As shown in Figure 3.8, the oil recovery ratio increased from 7.3% to 9.0% and the water cut fell to 90% from 100% when 0.3PV polymer was injected then increased to 97% during subsequent 0.1 PV injection. The reason why the change happened in RF and FW was because polymer

solution increased the viscosity of the displacing fluid and decreased the mobility ratio of water to oil. Therefore, the 2 macroscopic displacement efficiency was improved, and consequently, RF and WC were changed. 1.1 PV of microgel was then injected after polymer flooding but there was no prominent change for both RF and WC curve as shown in Figure 3.8.

However, the pressure shown in Figure 3.9 increased distinctly from 1.32 psi to 484.9 psi. This pressure growth may owe to gel particles placement in the pore spaces of sand grains or the gaps between the stainless pieces and core samples. After microgel

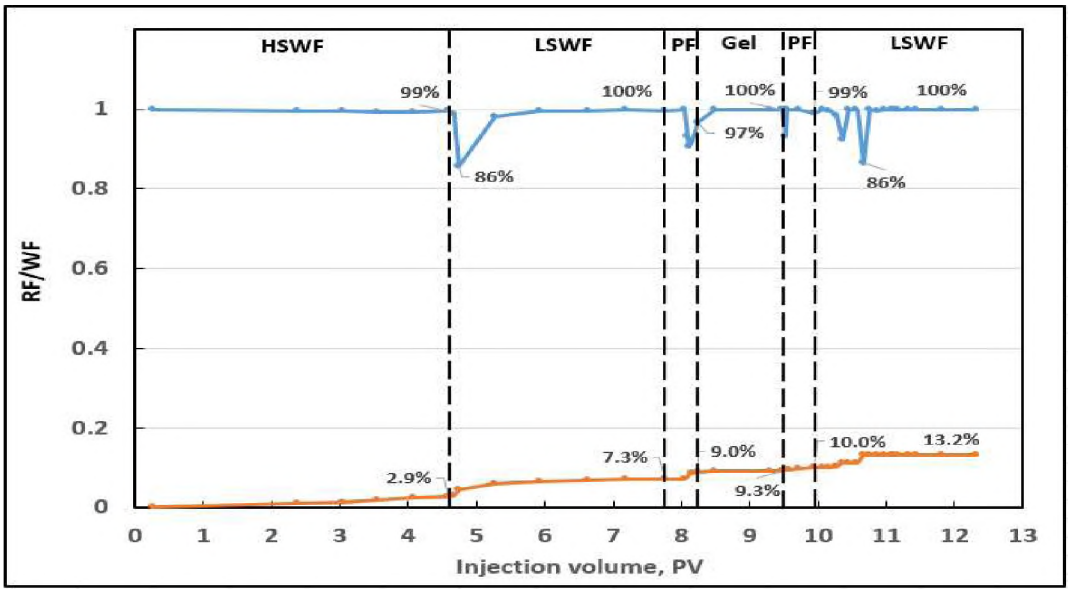

Figure 3.8 Oil recover ratio and water cut curves of DE-1.

flooding was finished, polymer flooding and low salinity water flooding were repeated to analyze the results after gel treatment. As shown in Figure 3.8, for the second polymer flooding process, the total injection volume was around 0.4 PV and the oil recovery ratio were only improved 0.7% compared to 1.7% increment for the first polymer flooding.

The reason why polymer flooding was not effective is that microgel plugging efficiency is not good enough to plug the pore spaces in sand grains to let polymer solution redirect to the surrounded matrix. This explanation can be verified from the water cut curve in Figure 3.8 and the pressure curve in Figure 3.9. As shown in Figure 3.8, the water cut kept descending but the decrease was only 1%. This phenomenon explained the saturated oil in the matrix was not being displaced by polymer solution. Besides, from the pressure curve in Figure 3.9, the pressure directly increased to the peak pressure of 1234.8 psi during the second polymer flooding process, which means polymer was being injected into high permeability zone to build up the pressure after gel breakthrough.

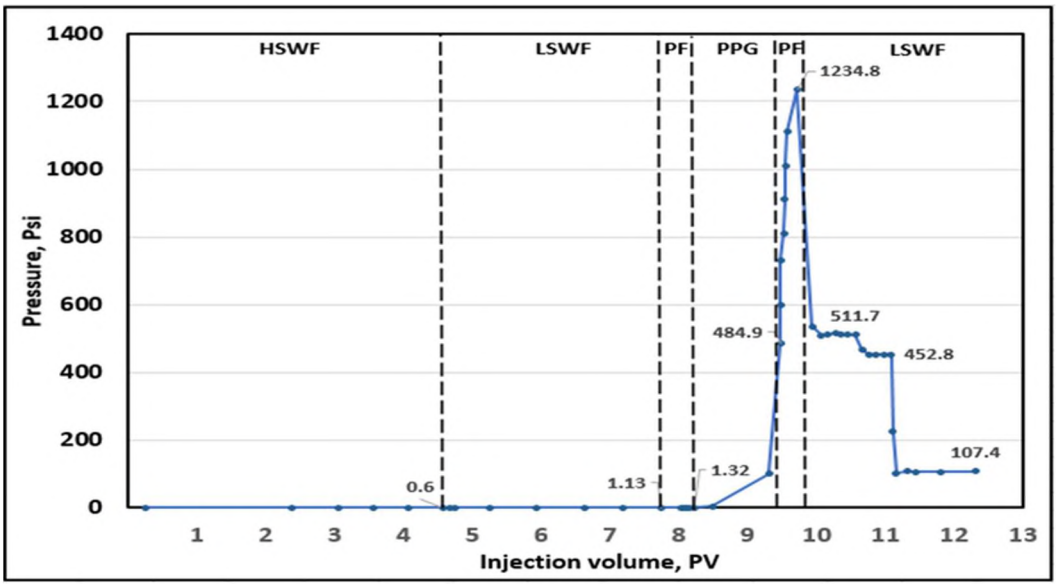

Figure 3.9 Pressure behavior of DE-1.

Finally, the pressure started to decrease as microgel was pushed out by polymer. During the second low salinity water flooding process, there were two RF increments

happened in first high and low salinity water injections, which were 1.2% and 2%, respectively. The corresponding water cut changes to these two RF increments decreased to 94% and 86%, separately. Both increases and decreases behaviors means water was redirected from high permeability zone to the low permeability matrix, and thus displaced more oil.

After low salinity water was injected, the pressure directly decreased to 511.7 psi and kept constantly about 0.5 PV injection time, then continually decreased to 452.8 psi for another constant 0.5PV injection time. Finally, the pressure decreased to 107.4 psi and stayed the same until the end of the injection. These three-pressure decrement and constant stages indicated that the injected microgel placement performance was not good enough as the microgel was still movable in high permeability zone.

The results of gel migration in lateral view and cross- sectional view of experimental model. The experimental model was taken out of the core holder after all flooding experiments were finished. As shown in the Figure 3.10, a denser and thicker gel cake was formed at the entrance of the core after gel injection process. The terminology of 'gel cake' in petroleum engineering refers to formation damage, which is embodied in terms of blocking the injection area to obstruct displacement liquid injection and increasing the injection pressure to a hazardous level. The formation damage results of gel cake were also reflected in the RF, FW and pressure cures in Figure 3.8 and 3.9. For the second polymer flooding process, the injection pressure increased dramatically but RF and FW value almost remained unchanged. This wasn't not only caused by inefficient microgel plugging performance but also the gel cake hindered polymer solution injection into the high permeability zone.

Figure 3.10 The lateral view of experimental model after all flooding experiments were finished.

The gel migration was illustrated in the cross- sectional view of experimental model in Figure 3.11. Almost all gel was injected into the gaps between the stainless-steel pieces and core samples instead of the medium black sand area, which demonstrated why RF and FW scarcely increased in the second polymer flooding process due to the model construction issue instead of the gel plugging performance issue.

Figure 3.11 The cross- sectional view of experimental model after all experiments were finished.

3.4.1.2. Discussion and modification of the first demonstrative experiment of microgel performance in sand filled fracture. *Discussion of DE-1.* Basing on the results described above, the design of experimental procedures is reasonable but the final recovery results are of un-satisfaction. As the results demonstrated, all procedures followed the experimental objectives, which included comparing the displacement efficiency of different salinity water and assessing microgel placement and plugging performance. In the different salinity water flooding experiments, the results are remarkable that the increment of oil recovery factor was 4.4% and the water cut decreased from 99% to 86% with no significant pressure growth. However, the gel placement performance is not good enough. Although there was no obviously RF and WF change during gel injection process which means the gel particle was not injected into matrix, the pressure still increased drastically. This result conformed to the observation in Figure 3.10 and 3.11 that the gel was not placed into the target area and the gel cake was formed to damage the formation. Therefore, for the gel plugging efficiency, despite the fact that oil recovery ratio was improved after gel injected, the results were not acceptable since the injected gel was not placed into the target areas.

Modification for next experiment. According to the prior discussion, in order to make the experiment results closer to a reasonable gel plugging and propagation performance in fractured channels, it is crucial to modify the experimental procedures and materials for next experiment. First, the low salinity water treatment is effective according to previous experimental results but the total injected volume (7.8 PV) is excessive, thus it is necessary to reduce the volume of salinity water below 1 PV. The reason why controlling the injection volume below 1 PV, it because the significant

variations of water cut is under nearly 1PV low salinity water injection in Figure. 3.8. Second, since the gel was injected into the gaps between core samples and stainless-steel pieces, Epoxy is necessary to use to block the gaps as shown in Figure 3.12. Third, for the purpose of simulating the real oil field flooding process, oil saturation after filling sand in fracture will be processed. Fourth, as the final oil recovery results were unsatisfactory, choosing higher permeability core samples may improve the results by making the displacing flood much easier to be injected into the matrix than using lower permeability core samples. Finally, stop injecting the microgel when pressure reaches around 1000 psi and check whether the gel will be produced since there was no gel was produced when the pressure reached 484.9 psi during the previous gel injection process and in the study of the application of PPG in super K (Imqam et al. 2015), the pressure that the gel has been produced from effluence is around 1000 psi under same pressure level in unit foot.

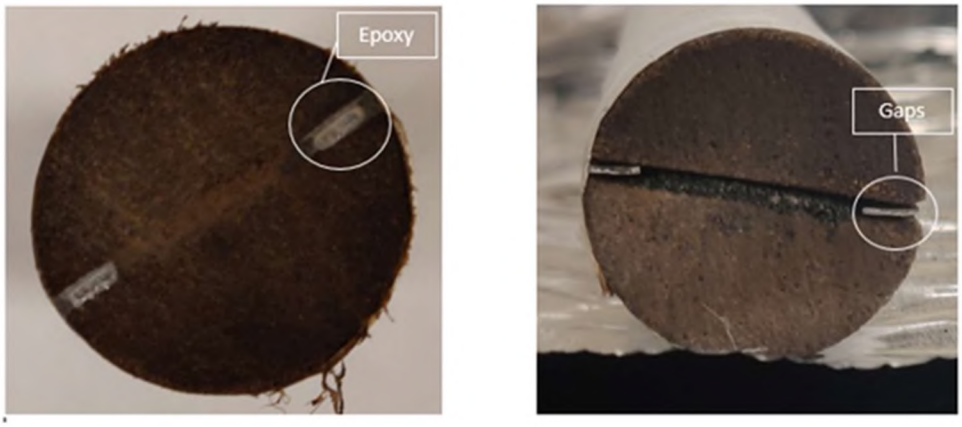

Figure 3.12 Using epoxy to blocking the gaps between core samples and stainless-steel pieces.

3.4.2. The Results of Second Demonstrative Experiment. The below content covered the results and modification of the second demonstrative experiment after the first experiment modification.

3.4.2.1. Second demonstrative experiment of microgel performance in sand filled fracture (DE-2). The design of the experiment procedures had already been established in the last experiment. Thus, the second demonstrative experiment would follow the first experiment procedures and do the study of experimental model preparation to check whether adopting epoxy to seal model works or not. The water cut, oil recovery ratio, pressure behavior and gel particle produced were shown in Figure 3.13, 3.14 and 3.15 as below.

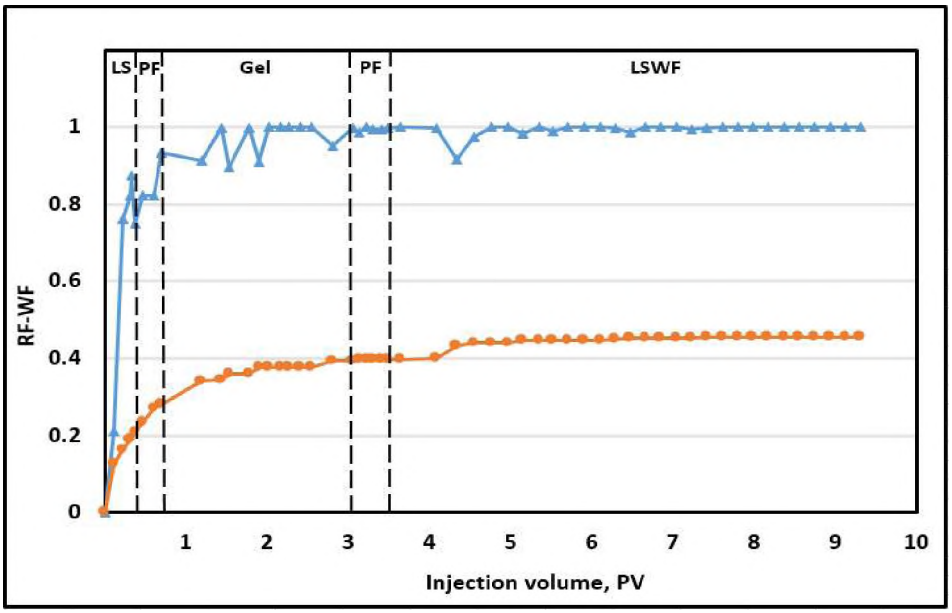

Figure 3.13 Oil recover ratio and water cut curves of DE-2.

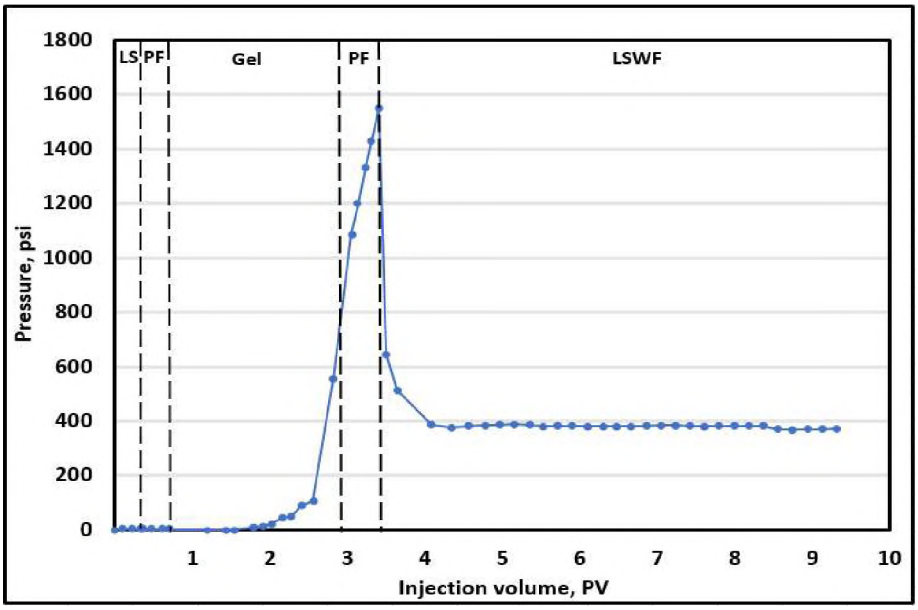

Figure 3.14 Pressure behavior of DE-2.

Figure 3.15 Gel particles produced during the second polymer solution injection.

The results of water cut, oil recovery ratio, and pressure behavior. For the first low salinity water and polymer flooding process, the injecting pressure kept staying at a

lower value which is around 2.5 psi, which is caused by the high permeability property of sand filled facture. The oil saturated in the filled sand was displaced by 0.4 PV low salinity water and 0.4 PV polymer solution. At the end of low salinity water flooding process, the oil recovery ratio increased to 19.4% and water cut reached 87.5%. For polymer flooding process, the oil recovery finally increased to 27.9% and the water cut decreased from 87.5% to 75% during first 0.05 PV injection and then increased precipitously to 93.3% during following 0.35 PV injection. The decrease of the water cut is because the macro displacement efficiency was improved by the increased viscosity of the displacing fluid. For the gel injection process, the total volume of gel injected was around 2.35 PV and 11.2 FPV, and at the end of gel injection process, the water cut, oil recovery ratio and pressure were approximate 99%, 39.5% and 1088.5 psi respectively. The water cut curve in Figure 3.13 revealed this gel performance process was more complex and hid a few potential problems than it appeared, specifically during the whole gel flooding process, the water cut curve was like zigzag shape, which fluctuated between 90% to 99% during first 0.8 PV injection and then kept 99% until the end of gel injection. Correspondingly, the pressure gradually increased first and then decreased steeply. Thus, based on the curve's behavior above, there were two possible problems hiding in gel flooding process. One is the gel mesh size selection problem that the 120-230 mesh size will cause the gel particle sizes in a wider range so that only the smaller gel particle will be placed into the pores spaces in sand grains while the larger gel particle would cumulate around the front face of experimental model and form the gel cake. As a consequence, the pressure increased firstly at a slow pace and water cut decreased

gradually, then finally increased sharply due to the gel cake formed by the larger gel particles.

The other problem is the filled sand hadn't been packed tightly enough before conducting the experiment. During the gel flooding experiment, loosened sand was repacked by gel particle firstly, and at the same time, due to the repacking process and the flow ability of sand, the pore spaces between sand grains will be compressed and oil droplets will be squeezed out. As a result, the water cut fluctuated and pressure increased gradually as shown in Figure 3.13 and 3.14. However, when the sand was repacked tightly enough, the injection pressure was not sufficient enough to let microgel to be injected into pore spaces. From this time, the pressure built up sharply until the pressure was high enough to let the gel particle to be injected successfully as shown in Figure 3.14. After the gel flooding process, the second polymer flooding and water flooding will be processed. The final oil recovery ratio is about 45.5% and the injection pressure was kept 372.2 psi constantly. During the process of second polymer flooding, the pressure firstly built up to 1549.2 psi approximately when the polymer solution was injected to 0.27 PV as shown in Figure 3.14. Then, the pressure fell off happened because the gel particle was produced by injected polymer solution. Finally, the pressure stopped at 648.4 psi when polymer solution injection was stopped. And gel particles produced during the second polymer solution injection was shown in Figure 3.15. As a contrast, there was no significant change happened for water cut and oil recovery ratio during the whole polymer flooding process. In the following secondary water flooding process, the total injected volume of low salinity water was around 5.7 PV. The pressure decreased from 514.7 psi to 372.2 psi and the oil recovery ratio increased from 39.8% to 45.4%. There

was a conspicuous variation in pressure, RF and FW curves when the low salinity water injection reached 0.92 PV. In this visible variation, the pressure decreased from 514.7 to 382.7 psi, the water cut decreased from 99% to 91% and the oil recover increased from 39.8% to 43.2%. The reason why this variation happened was that even the gel plugging performance was not good enough as the second polymer flooding, because some of the gel particles still been placed in the medium, which would result in decreasing the permeability of sand filled area.

The results of gel migration from lateral view and cross- sectional view of experimental model. After finishing all experimental procedures, the experimental model was taken out and open using blade followed the area sealed by epoxy. Figure 3.16 displayed the cross- sectional view of experimental model after incision. As shown in Figure 3.16, from the right-side inlet to left side outlet, the distribution of the white gel reduced gradually and the shape of gel migration was like penetrating the sand area instead of filling in the spaces between sand grains homogeneously. The aforementioned gel migration and distribution demonstrated the potential problems mentioned previously truly existed during the gel flooding process that the abnormal water cut curve in gel flooding process was caused by loosen filled sand and the large gel size range difference. The loosen filled sand issue could be observed from gel migration shown in Figure 3.16. For an idea gel migration, the gel should be injected into the pore spaces between the sand grains uniformly. However, the result shown in cross-sectional view in figure was significantly different. The gel particle created a channel by pushing the sand from the middle to the side and then followed the channel to migrate. Thus, the phenomenon that the sand was pushed by gel demonstrated the sand compaction was not tight enough. In

contrast, if the sand was compacted well, the gel would be injected into the spaces between sand grains. For another issue, the large gel size range difference can be detected by the distribution of micro gel from the cross view shown in Figure 3.16. As Figure 3.16 illustrated, the distribution of micro-gel from right to left also reduced gradually. This reduction behavior was caused by the earlier breakthrough of the smaller size gel particles in the sand area than that of the larger size gel particles.

The pressure kept building up as the gel cake was formed by larger size gel particles remained at the surface of injection area in the Figure 3.17. When the pressure increased to the break through pressure of larger size gel particles, the larger size gel particles where been injected into the sand area where pre-occupied by smaller size gel particles. Consequently, most of the smaller size gel particles were displaced out by larger size gel particles earlier and most of the larger size gel particles were trapped in the sand area at current injection scenario.

Figure 3.16 The cross-sectional view of experimental model after all procedures were finished (The brown color means sand and white color means gel particle).

Figure 3.17 The lateral view of experimental model after all procedures were finished.

3.4.2.2. Discussion and modification of the second demonstrative experiment of microgel performance in sand filled fracture. According to the results of the pressure and cross-sectional view figures, the average pressure before and after gel flooding in DE-2 is higher than the pressure in DE-1, which means the gel can be injected into the target area even the gel distribution and migration were not non-ideally. Therefore, this experiment successfully achieved the experimental objective which is to set up an optimized experimental model by using epoxy to seal the gaps between the gaps of the steel spacers and core samples. However, the gel performance was still not good enough.

The water cut curve behaved unreasonable compared with other gel flooding experiments (Goudarzi et al., 2015). Two possible issues have been demonstrated; one was the compaction of filled sand was not tight enough and the other one was that there was a larger size difference for the selected sand. The increment of oil recovery ratio was also not ideal due to the unreadable gel performance. Although the pressure built up to

more than 1500 psi when gel break through happened and the final oil recovery ratio was 38.5% when the final pressure was only kept constant around 380 psi, this final oil recovery ratio was not convincing in terms of the gel plugging efficiency because the water cut before gel flooding process haven't reached over 95% yet. In other words, before the gel injection, the displacement potential was not been expended completely so that some pre-saturated oil can still be displaced in filled sand area when the gel plugging efficiency was well enough during gel injection.

Modification for next experiment. Based on the discussion above, two modifications should be applied in next experiments. The first one is setting the water cut to nearly 99% at the end of low salinity water flooding. The aim of this modification is to extend all displacement potential of experimental model before gel flooding process and leave the least amount of the oil in the matrix. The second one is focusing on solving two issues that were loose compaction of filled sand and larger average gel size. Thus, the modification of next experiment will not only find the solution of the trouble in gel flooding process but will also prove the existence of these two issues. Therefore, the second modification for next experiment is processing the same experimental procedures as DE-2 but stopping gel injection when the injection pressure reaches around 10 psi since the gel injection pressure started to build up sharply and the water cut started to perform unreasonable when the pressure was around 9 psi. It is also unclear of the gel migration and distribution before 9 psi based on the DE-2 results. For this reason, the second modification in next experiment will play an important role for following experiments in terms of solving and detecting experimental issues.

In conclusion, there are two modifications in next experiment, which include:

1. Do not stop first low salinity water injection until the water cut reaches 99%.

2. Repeat the DE-2 experiment procedures completely the same but stop gel injection when the injection pressure reaches around 10 psi.

3.4.3. The Results of First Gel Application in Alaska Sand Filled Fracture.

The below content covered the results and modification of the first gel application in Alaska sand filled fracture experiment after the demonstrative experiment modification. And the modifications includes controlling the shutdown water cut and pressure of first water flooding and gel treatment respectively.

3.4.3.1. Experimental results of microgel placement and plugging performance in Alaska sand filled fracture (MPA-1). The objective of the last experiment is to test whether using epoxy to seal the experimental model will work in terms of letting gel particles be injected into the target area. Based on the experimental results, the objective had been achieved but the gel performance was not acceptable, which in terms of gel migration, distribution and plugging performance. The reasons why gel performance was terrible were due to two issues conjectured from the results, which are filled sand compaction issue and huge difference in gel sizes. Thus, the purpose of this experiment is to verify one of the issues, which is the filled sand compaction issue. The curves of oil recovery ratio, water cut and pressure behavior of the microgel placement and plugging performance in Alaska sand filled fracture were shown in the Figure 3.18 and 3.19.

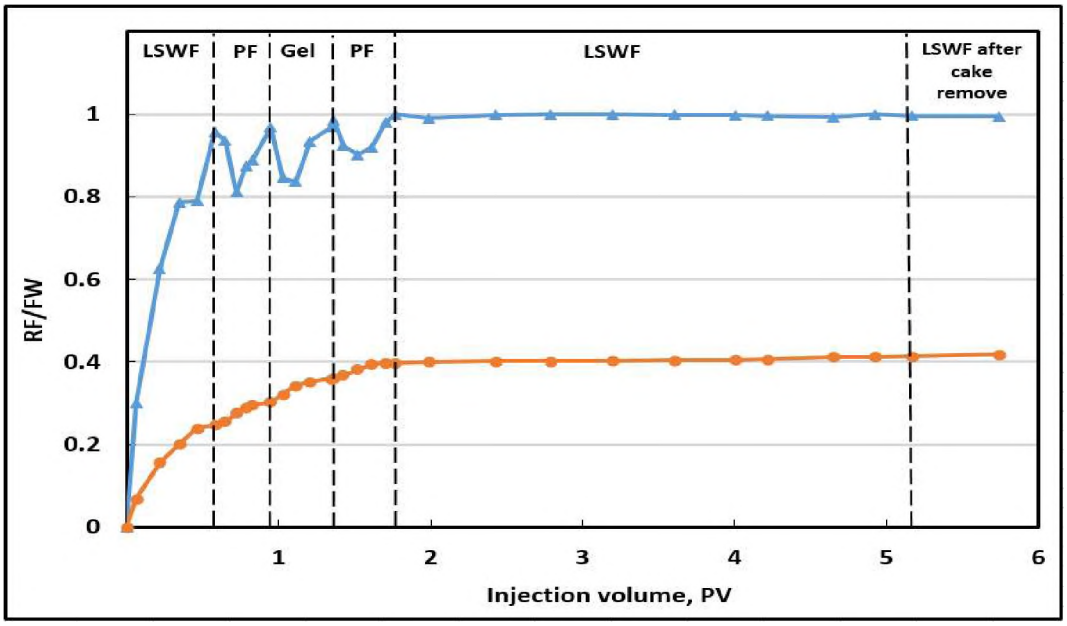

Figure 3.18 Oil recover ratio and water cut curves of MPA-1.

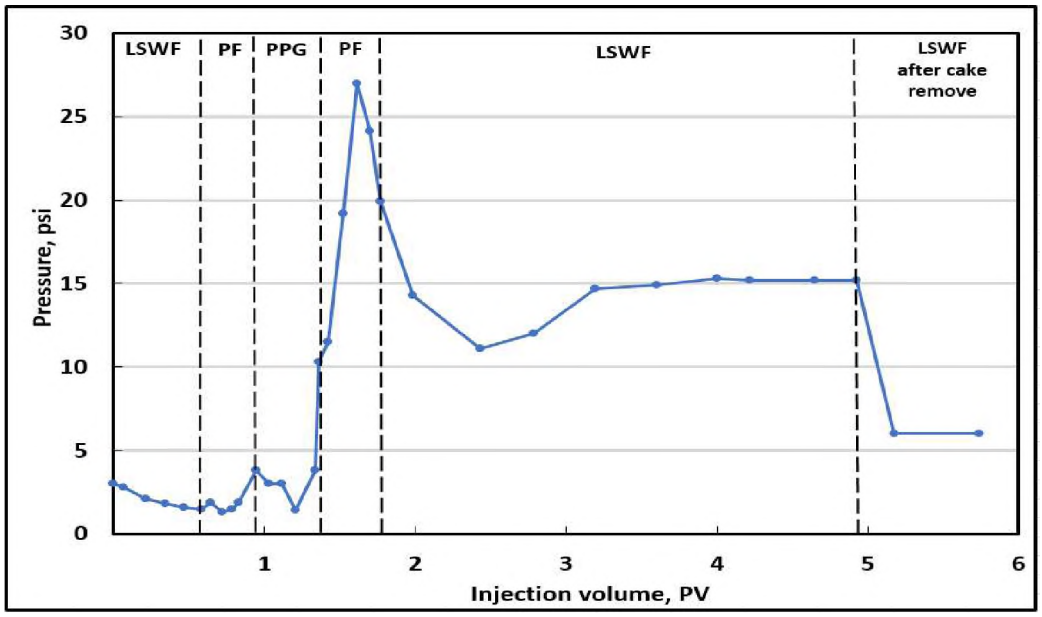

Figure 3.19 The pressure behavior of MPA-1.

The results of water cut, oil recovery ratio, and pressure behavior. As shown in the Figure 3.18 and 3.19, the experiment of MPA-1 still processed the same experimental

procedures that were conducting water and polymer flooding before and after gel flooding. For the results of water and polymer flooding before gel flooding, the total volume of water and polymer injection were 0.58 and 0.4 PV and the final water cut at each end point of flooding process were 95.7% and 96.8 with corresponding oil recovery ratio of 24.8% and 30.2%. The water cut value at each ends of flooding process had already coincided with the modification in this experiment that is setting the water cut around 95% before gel injection. These two higher water cuts mean the potential for oil being displaced had been significantly decreased, which was a positive sign and good timing to evaluate gel performance next. For the following gel flooding process, the total volume of gel injection was 0.05 PV when pressure increased to 10.3 psi. During this gel injection process, the water cut curve performed an acceptable result that decreased to around 83.7% from 96.8% for the first 0.1 PV injection and then increased to nearly 97% for the followed 0.3 PV injection. Correspondingly, the oil recovery ratio increased from 30.2% to 36%. However, just basing on the RF and FW results can not verify whether the gel performance is good enough. The cross- sectional view would provide more convinced results as shown in Figure 3.20. During the next secondary polymer flooding, after 0.4 PV of polymer was injected, the pressure built up to around 27 psi then decreased to approximate 17 psi, which leads to oil breakthrough and oil recovery ratio increased from 36% to 39.7%. However, the RF and FW results alone cannot demonstrate the true displacement condition in the experimental model. The experimental model photos were still need to be combined with the RF and FW results to judge. Finally, for the second water flooding, there were no obviously changes for the water cut

and the oil recovery ratio because there was hardly any oil remained in the channel after displaced by polymer solution.

The results of gel migration in lateral view and cross- sectional view of experimental model. After all experimental procedures were finished, the experimental model was taken out from the core holder and opened by following the middle area where was sealed by epoxy and the cross- sectional view of experimental model after opened was shown in Figure 3.20. First, within the red-dashed circle, from the right-side inlet to the left side outlet, it was obvious to observe that some gel particle had been injected into the sand area. However, the injected gel particles were assembling as a mass and occupying some areas separately in the fracture instead of distributing between the sand grains uniformly. Thus, from the aforesaid phenomenon, it was no doubt that the issue which the filled sands were pushed and repacked by the injected gel particles was demonstrated and the reason that the filled sands were repacked was the compaction of filled sands were not tight enough. Second, the phenomenon that the filled sands were repacked by gel particles can explain why the water cut decreased and oil recovery ratio increased during the gel injection process. Since the filled sands were repacked, the spaces between the sand grains would be reduced so the oil drop would be squeezed out, and as a result, the RF and FW increased. Third, in accordance with the gel migration and distribution in cross-sectional view of experimental model, the water cut and oil recovery ratio changed in second polymer solution flooding could be explained. Though the gel plugging was failing as the gel particles assembled as a mass and occupied some area in the fracture instead of being injected into the spaces between the sand grains, this mass of gel could still play a role of plugging the fracture and reducing the permeability of sand

filled fracture. Specifically, during the next polymer flooding, the polymer solution first broke through the gel cake formed near the inlet and then diverted to the matrix instead of being injected into sand filled area due to the gel mass effect. Thus, the oil in the matrix were displaced during the period of polymer solution redirection. Finally, after the polymer solution finished the displacement process in the matrix around the gel mass area, the polymer solution was diverted again to middle sand filled fracture area with not much oil being displaced. Thus, the water cut reduced and oil recovery ratio increased in second water flooding.

As reflected in Figure 3.21, the formation damage phenomenon still appeared where a broken gel cake was formed after the experimental model was taken out. Comparing with less gel remained on the sides of experimental model, most of gel remained on the surface of inlet. Due to lack of equipment to analyze the gel cake, it is hard to measure how much the gel formed the gel cake but more gel cake analyzations will be recorded in later results discussion.

Figure 3.20 The cross-sectional view of experimental model after all procedure finished.

Figure 3.21 The lateral view of experimental model after all procedures were finished. a) the experimental model, the brown color means matrixes and white color means gel particles. b) the inlet injector, the silver color means the surface of injector, the white color means the gel particle.

3.4.3.2. Discussion and modification of microgel placement and plugging performance in Alaska sand filled fracture. Comparing the results of MPA-1 and MPA-2, even though the experiment MPA-1 followed the same procedures and used the nearly same material as the experiment DE-2 the RF and FW curves still performed the obvious difference in terms of changing trend.

One of the reasons in curves trending differences was the sand filling condition difference. The same weight of two kinds of sand can just guarantee the volume that was filled in the fracture was same but it is difficult to ensure the equal interactions between sand and sand, sand and water, and sand and oil. Thus, the sand filling condition is one reason to cause the differences between the curves of RF and FW curves in MPA-1 and DE-2. Second, before the gel flooding process, the changing trends of FW in two experiments were the same, both waters cut sharply increased in water flooding and met an obvious decrease during 0.1 PV polymer solution injection, then increased gradually

in followed 0.3 PV polymer solution injection. At the same time, the average incremental oil recovery ratio was 6.5% during the polymer flooding process. However, the end points of two flooding process in two experiments were different. At the end of water flooding, the oil recovery ratio and water cut were 24.8% and 95.7% respectively in MPA-1 but were 20.7% and 88% in DE-2. At the end of polymer flooding, the water cut and oil recovery ratio increased to 96.8% and 30.2% respectively in MPA-1, yet they increased to 93% and 27.9% in DE-2. From the results difference above, the modification in MPA-1 that setting the water cut around 95% in first water flooding was successful as the final water cut (96.8%) and oil recovery ratio (30.2%) before gel injection were both higher values than those of the results in DE-2. Thus, the objective of expending the potential energy of displacement before gel flooding was achieved. Third, during the gel flooding process, the pressure of two experiments built up to around 10 psi when the gel injection volume was 6 PV. However, the increment of oil recovery ratio is significantly different, which were 5.8% and 11% in MPA-1 and DE-2, respectively. The reason why the RF in DE-2 was higher than in MPA-1 was that the potential energy of displacement has been expended before gel flooding in MPA-1 so that it is harder to produce more oil when gel flooding processed. In addition, the reason why the zigzag water cut curve did not appear in MPA-1 was mainly caused by the different sand filling condition that was mentioned before. From the Figure 3.20 it was no doubt that the sand was repacked by gel particles. Considering the sand filling condition and the remaining oil in sand area were different in two experiments, the sand grains in experiment DE-2 had more spaces and chances to be repacked when the gel particles were injected to form a zigzag curve in DE-2. In contrast, less oil remained and larger inter-particle cohesion in the sand area

would lead to less spaces and chances to cause sand repackage so there was no zigzag curve during the gel flooding process in MPA-2 experiment. Fourth, an obvious water cut decrease happened in second polymer flooding in MPA-1 experiment instead of DE-2 experiment. In DE-2 experiment, the thicker gel cake as shown in Figure 3.21 had totally blocked the injection area of the experimental model. As a result, the pressure built up sharply and breakthrough happened. However, as shown in Figure 3.25, the thinner gel cake did not blocked injection area of experimental area thoroughly so the polymer solution can be injected and redirected that has been explained in cross-sectional view result part. For the last secondary water flooding part, since there was no gel breakthrough phenomenon happened, the condition in sand filled area kept constant and oil was not been produced so much.

Comparing the lateral view of the experimental model in Figure 3.21 and 3.25, since the total injection volume of gel in DE-2 experiment is higher than that of MPA-1 experiment, a denser and more complete gel cake was formed in DE-2 experiment. caused a higher breakthrough pressure level up to 1500 psi in second polymer flooding process. In contrast, the sparser gel cake that was formed in MPA-1 experiment only caused a lower breakthrough pressure that is around 27 psi in second polymer flooding. Although two breakthroughs happened apparently in two widely different pressure level, yet the flow behaviors of displacement fluids inside the experimental models were fundamentally different. For the 1500 psi breakthrough pressure experiment due to the denser gel cake, the breakthrough happened when the injection pressure was high enough to let the gel to break through the gel cake and then the gel spurted into the sand filled area and produced finally by penetrating the sand area. This breakthrough behavior also

verified why no more oil was produced during the polymer flooding. The polymer solution played a role of building up the pressure, and when pressure breakthrough happened, the polymer along with the gel were being injected into sand filled area instead of diverting to the matrix as no more oil was produced in polymer flooding. For the 27psi breakthrough pressure experiment due to the sparser gel cake, the pressure breakthrough happened when the injection pressure was high enough to let the polymer solution to break through the gel cake. Then the polymer solution was diverted to the matrix due to the gel mass effect and finally some saturated oil in the matrix will be displaced by polymer solution.

To sum up, the results of DE-1 and MPA-2 experiments were compared. First, the issue that gel particle repacked the filled sand in early period of gel flooding had been confirmed. Second, the dramatically pressure build up was caused by the gel cake formed and blocked subsequent injection fluid.

Modification for next experiment. Based on the discussion above, although the sand repackage issue had been demonstrated, whether a huge gel size difference is one of reasons to cause this issue still needs to be verified. Specifically, when there is a huge difference in injected gel sizes, only a few of smaller size gel particles will be injected into the spaces between the sand grains while most of gel particles will still remain in injection area and then repack the filled sand area. Consequently, the gel cake will be formed by these remained gel and block subsequent injected fluid and the pressure will build up sharply. However, the gel size difference is just a conjecture that cannot be proved based on current results.

To verify whether a huge difference in gel sizes is one of the reasons to cause issue that the gel repacks the filled sand, the modification of next experiment should be as follow: Reduce the gel size upper limit from 120-230 to 170-230 mesh during the gel flooding process, and checking whether a huge difference in gel sizes is one possible reason to cause issue that the gel repacks the filled sand.

3.4.4. The Results of the Second Gel Application in Alaska Sand Filled Fracture. The below content covered the results and modification of the second gel application in Alaska sand filled fracture experiment after the modification of first gel application in Alaska sand filled fracture experiment.

3.4.4.1. Experimental results of microgel placement and plugging performance in Alaska sand filled fracture (MPA-2). In the last experiment, the results had demonstrated that loose compaction of filled sand is one of the issues to cause unreasonable gel performance in the early period of the gel flooding process. However, whether the larger sand size or a huge difference in sand sizes is another issue to cause the unreasonable gel performance had not been verified. Thus, in this experiment MPA-2, by reducing the lower limit of the gel size in terms of selecting the smaller size gel to verify the issue and check whether smaller size gel could mitigate the sand repackage issue and enhance the gel performance. The below Figure 3.22 and 3.23 have illustrated the results of oil recovery ratio, water cut and pressure behavior.

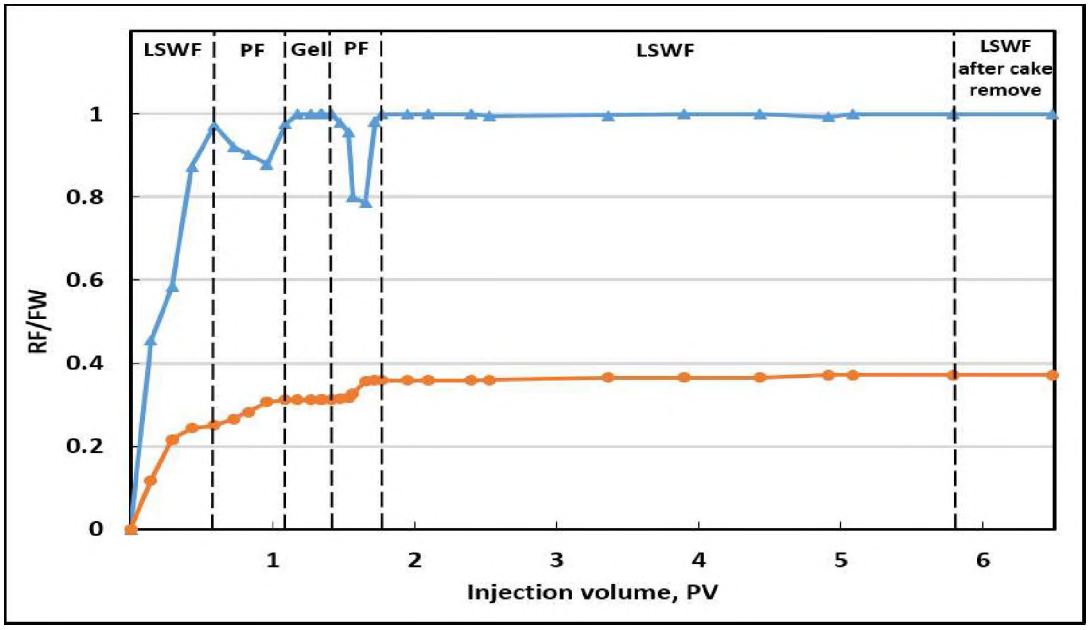

Figure 3.22 The water cut and oil recovery ratio results of experiment MPA-2.

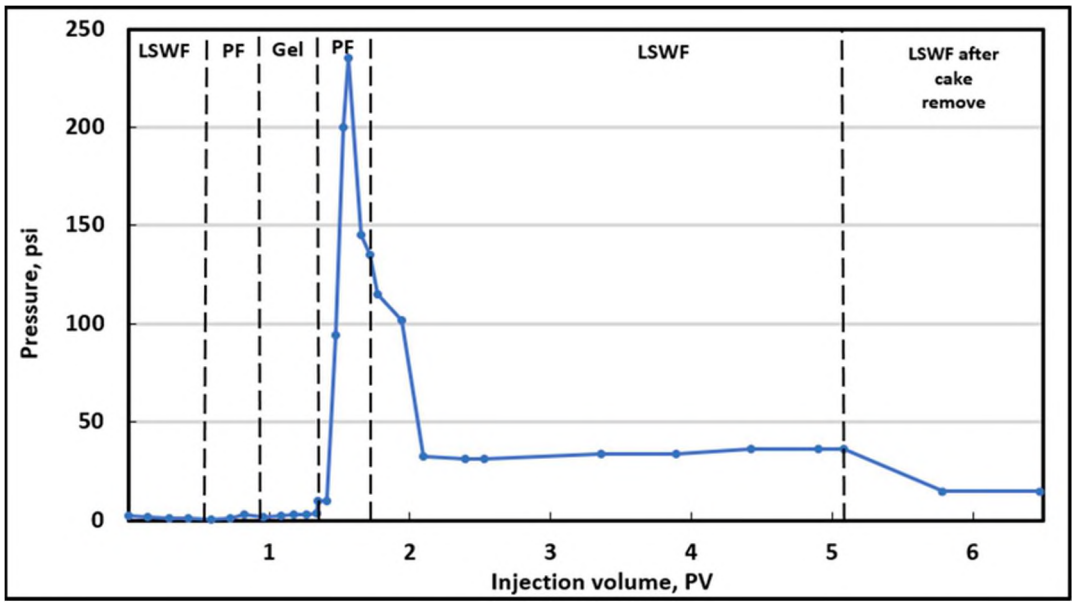

Figure 3.23 The pressure behavior of experiment MPA-2.

As shown in Figure 3.22, both the water cut at the end of water flooding and polymer flooding reached around 97% and the oil recovery ratios were approximately

25% and 31% correspondingly. In addition, before the injected volume of polymer solution was 0.35 PV, the water cut kept decreasing to nearly 87.8%. The reason why water cut decreased in the polymer flooding process is because the macroscopic displacement efficiency was increased by increasing the displacing fluid viscosity. However, in later gel flooding process, the water cut, the oil recovery ratio and the pressure kept constant until the injection pressure built up to 10 psi as shown in Figure 3.23.

In accordance with the cross-sectional view of experiment model as shown in Figure 3.24, the gel particles were evenly distributed in the channels between the sand grains. It meant the resistance when gel particles were injected was constant, thus the injection pressure nearly kept changeless during the gel flooding process. Moreover, the water cut at the end of polymer flooding had already reached approximated 97%, which meant there were not much oil remained in the between the sand grains when the gel particles were injected so the water cut and oil recover ratio kept constant through whole gel flooding process. In second polymer flooding process, there were obvious variations occurring in water cut, oil recovery ratio, and pressure curves. First, as shown in Figure 3.23, the pressure dramatically increased to 235 psi when the injected volume of the polymer solution was 0.2 PV. Then the pressure breakthrough occurred as shown in Figure 3.22, the water cut suddenly decreased to 78.6% when the injected volume of the polymer solution was around 0.31 PV and the pressure was kept at 145 psi. At the same time, the oil recovery ratio increased to 35.6%. Combining the cross-sectional view in Figure 3.24, the explanation of RF, FW and pressure change should be as follow. Before the 0.2 PV injection of the polymer solution, the polymer solution was blocked into the

experimental model due to the gel cake so the pressure built up. When the pressure reached the breakthrough pressure, the polymer broke through the gel cake and began to flow into the experimental model. Thus, during the 0.2 to 0.3 PV polymer injection, the polymer solution was diverted into the matrix and displaced oil because of the gel plugging performance. As a result, the water cut decreased sharply and the oil recovery ratio increased obviously. In the later 0.1 PV polymer solution injection, the polymer solution was diverted again to the middle sand filled area and the water cut increased to nearly 99% as no more oil was produced. Finally, in second low salinity water flooding, because most of the saturated oil had already been displaced by polymer solution, thus there was an inconspicuous change in water cut and oil recovery ratio curve with the pressure finally kept constant around 36 psi.

Figure 3.24 The cross-sectional view of the experimental model.

The results of gel migration in lateral view and cross-sectional view of the experimental model. For the results of the cross-sectional view, the results have been mentioned much enough in the last section, thus in the section there is no more result

analysis of the cross-sectional view. For the lateral view of the experimental model as shown in Figure 3.25, there was still a denser and intact gel cake formed. Even though the gel cake was divided into two parts when the model was taken out from the core holder, by observing the gel cake from the side view of model as shown in Figure 3.25 (a), this gel cake still covered on the side surface of model thoroughly. Thus, when pressure breakthrough happened, the polymer fluid must break through the gel cake and then flew into the experimental model. The higher breakthrough pressure was around 235 psi as shown in Figure 3.23.

3.4.4.2. Discussion and modification of microgel placement and plugging performance in Alaska sand filled fracture. *Discussion of MPA-2 results.* By comparing with the results of MAP-1, a particular discussion of MPA-2 results will be written down in this section by following the core flooding procedure, specifically as follow:

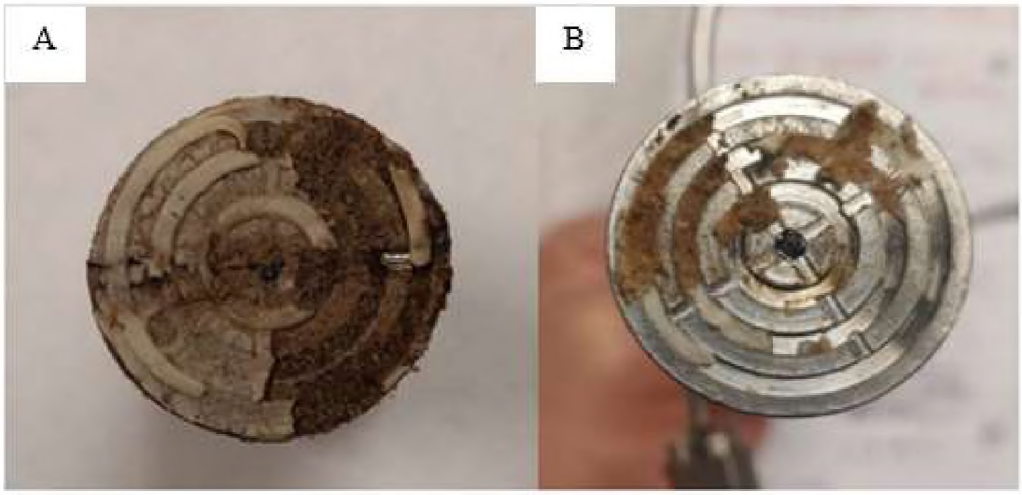

Figure 3.25 The lateral view of the experimental model.

In the first low salinity water flooding and polymer flooding process, there was no significant difference for the water cut and oil recovery ratio curves of two experiment results. In two experiments, both the water cut increased to approximately 97% at the end of the polymer flooding processes and oil recovery ratios reached around 30%. However, the average pressures were rarely different during water flooding and polymer flooding, which were 2.5 psi and 1.5 psi in MPA-1 and MPA-2, respectively. Yet, this smaller difference can be neglected due to the sensor error which has a wide range of 0-500 psi and he deviation of the sensor error is 5%. Thus, in accordance with RF, FW, and pressure results, the compacted conditions of filled sand in the fracture should be nearly the same. During the gel flooding process, an obvious difference had been found in the results of the gel flooding process between two experiments, and the evidence for the differences is adequate. First, the gel migration and distribution were distinct from the cross-sectional view of two experimental models. The gel with larger size played a role of repacking the filled sand in the experiment MPA-1 while the gel with a smaller size in MPA-2 had its intended effect of plugging the channels effectively. As shown in Figure 3.24, the gel particles with a smaller size were injected into the channels between the sand grains and distributed homogenously. Thus, the gel plugging performance was acceptable in the MPA-2 experiment. However, it was subjective if only the results were relied on the cross-sectional view. More convictive contributions were made in later discussions. Second, different from the RF and FW changes in the MPA-1 experiment, they kept constant during the gel flooding process in the MPA-2 experiment. This curve performance is the same as the gel flooding in a conventional open fracture (Xindi et al., 2018). Thus, the RF and FW curve behaviors in the MPA-2 experiment were reasonable.

Besides, the reason why there was no any oil been produced during the gel flooding process in MPA-2 experiment was caused by the gel particle been injected into the channels between the sand grains as shown the Figure 3.22 and the water cut had already reached a high level at the end of previous polymer flooding. Therefore, no more oil drop was squeezed out by sand repackage or gel particle displacement. Third, as the discussion for MPA-1, when the sand repackages issue appended, the pressure will fist decrease to below 2 psi and then increase sharply to 10 psi during the gel flooding process. However, in the MPA-2 experiment, the pressure nearly kept constant at 3 psi before pressure abruptly increased to 10 psi. Hence, this pressure behavior in the MPA-2 experiment demonstrated again that the gel had been placed into the channels between the sand grains. Besides, combining the cross-sectional view and the pressure behavior during the gel flooding process, the migration of the gel particle during the gel injection process could be explained as follows. At the beginning of the gel particle injection, the smaller size gel particles would be injected into the channels between the sand grains and the larger size gel particles would remain on the injection area and cumulate to form the gel cake. The pressure kept low and constant at this time. When enough dense gel cake was formed, the following gel injection would be blocked and pressure built up sharply. Finally, the total volume of injected gel particles in MPA-2 experiment was 4PV, which is lower than 6 PV of the MPA-1 experiment. When the injection pressure reached the same level, lower injection volume means the placed gel volume is also lower. Thus, the total gel volume placed in MPA-2 experiment was lower than that of MPA-1 experiment, in other words, the smaller gel volume was injected into the channels without repacking the filled sand. In the second polymer flooding process, the gel plugging performance

was acceptable in reference to the results in the last section. First, the overall changing trends of water cut and oil recovery ratio curves in MPA-1 and MPA-2 experiments were similar. However, the variation in the curves was significantly different. The water cut decreased from 99% to 83.7%, and the oil recovery ratio increased from 31.1% to 35.9% in experiment MPA-2. In contrast, the water cut decreased from 96.8% to 92.3% and oil recovery ratio increased from 36% to 39.1% in experiment MPA-1. The reason why the different variation happened between two experiments can be explained by the cross section view in two experiments, just as the analyzation above, under the same pressure level, the gel propagations are different, the effective gel plugging area in the Figure 3.24 is larger than in Figure 3.20, thus the volume of polymer solution diverted into the matrix was higher in experiment MPA-2 and more oil was produced in experiment MPA-2. Overall, the gel plugged performance or conformance control in experiment MPA-2 was better than experiment MPA-1. Second, the breakthrough pressure (235 psi) in experiment MPA-2 was nearly 9 times higher than the breakthrough pressure (27 psi) in experiment MPA-1. The higher breakthrough pressure meant the plugging efficiency is better, which could be explained as the plugging performance is better. As a result, the reduction of permeability was prominent, and thus a higher-pressure level occurred when a breakthrough happened.

In the final low salinity water flooding process, compared with the pressure behavior in experiment MPA-1, the injection pressure in experiment MPA-2 kept higher and steady. The stable pressure behavior indicated the gel placed well between the sand grains; in other words, there was barely gel transportation in the filled sand area. The

higher-pressure behavior verified again that the plugging performance with smaller size gel worked better than the larger size gel.

To sum up, smaller size gel played a crucial role in terms of improving sand repack issue and plugging performance compared with larger size gel.

Modification for the next experiment. On the basis of all previous experimental results and discussion, the terrible gel performance caused by two issues which are loosened compaction of the filled sand larger differences in sand sizes range has been confirmed. Thus, it is necessary to select the smaller size gel to finish the experiment and try to use tools to compact the sand as tightly as possible. It is feasible the experiments are modified along the two mentioned lines but these modifications are so vague that it will take a long time to verify the best solution to set up a workable and mature experimental mode. For this reason, the paper SPE- 89468- PA provided some specific and valuable size of the gel. The gel sizes selected in this paper were below 230 mesh sizes. Besides, a type of softer gel particle with the swelling ratio of around 60 times was selected. The reason for using the softer gel was because the swelled gel particle can deform and pass the channel as shown in Figure 3.26. Moreover, a larger size mesh sand was selected in this paper, 30-40 mesh size.

Therefore, these modifications should be included in the next experiment, as follows:

1. Change the gel type with the swelling ratio from 20 times to 60 times.
2. Select the gel size below 230 mesh size.
3. Change the sand size from 60-80 mesh size to 30-40 mesh size. Since the silica

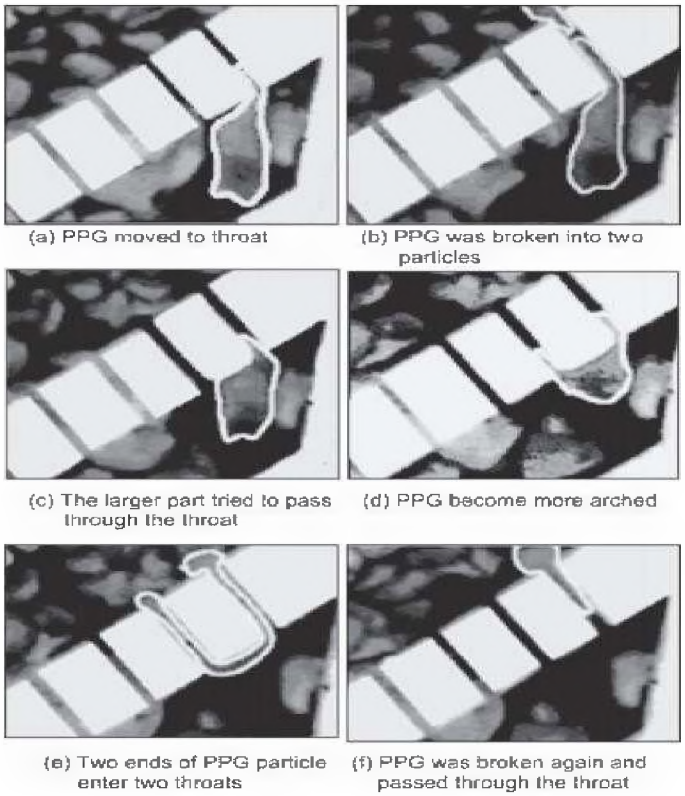

Figure 3.26 A process of a particle transporting through the channel at the simplified model.

sand size provided by Alaska oil field was 60-80 mesh size, the commercial silica sand with 30-40 mesh size will be used instead of Alaska sand.

4. Dye the gel with PH neutral dye to trace and object the gel migration and distribution in the filled sand area. The dye result was shown in Figure 3.27.

By following the above modification in the next experiment, the objective of the next experiment is to check the gel performance in terms of gel migration and distribution and whether the sand repackage issue happened again.

Figure 3.27 The micro gel before and after dye.

3.4.5. The Results of the Gel Application in Commercial Sand Filled Fracture without Core Flooding Process. According to the results and discussions in previous all experiment, two issues that caused the unreasonable gel performance had been confirmed. One issue is loose compaction of filled sand and the other one is the negative impact of injecting larger size gel particle. Thus, by following the verified issues above and the parameter provided in paper SPE- 89468- PA, some modification will be made in terms of tightening the sand by using tools, selecting smaller size gel to inject and choosing a softer gel. Therefore, the objective of this experiment MPC-0 is to finish a macroscopic experiment that is just processing gel injection instead of whole core flooding procedures to observe and evaluate the gel place performance in the sand filled fracture after modification.

3.4.5.1. Experiment results of microgel placement and plugging performance in commercial sand filled fracture (MPC-0). *The results of gel migration in lateral view and the cross-sectional view of the experimental model.* The gel

injection was stopped as soon as the gel particle was produced. Then the experimental model was taken out from the core holder and followed the meddle sealed epoxy to open the model. The cross-sectional view of the experimental model was shown in Figure 3.28. As shown in Figure 3.28, the gel placement performance was acceptable. First, by observing the whole cross-sectional view of the experimental model, the gel particle which was dyed in purple had been placed in whole channels between the sand grains after gel injection. Moreover, from the right inlet to the left outlet, the gel distribution decreased gradually by inspecting the variation in the shades of color. In addition, to demonstrate this decrement of gel distribution, a bottle test was introduced. As the color distribution in Figure 3.28, The dying gel was mainly concentrated at top 1/4 and last 3/4 area of sand.

By removing the top 1/4 and last 3/4 area gel mixtures and placing into two bottles and then centrifuging to check the gel volumes in two bottles. The centrifuging results were illustrated in Figure 3.29, which shows the gel volumes were nearly same for both top 1/4 and last 3/4 mixtures. Thus, it was proved that the gel distribution reduced progressively from the inlet to the outlet.

Figure 3.28 The cross-sectional view of the experimental model.

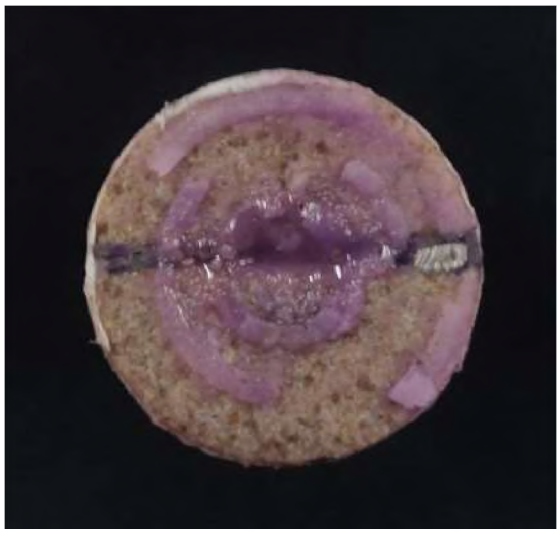

Figure 3.29 The lateral view of the experimental model.

For the lateral view of the experimental model in Figure 3.30, a fragmentary gel cake was formed. Based on the variation in shades of color, the gel particles in the gel cake mainly concentrated at the middle area within which is the inlet of the sand filled high permeability area. In contrast, on the side surfaces of the matrix, the concentration of gel particles was lower as the gel cake was not integrated enough to cover the whole matrix side surfaces. The above-mentioned gel cake behavior was reasonable because the gel mainly concentrated on the inlet of sand filled high permeability area instead of the side surface of matrix, which indicated the later displacing fluid was easy to break through the gel cake and apt to be diverted to flow into the matrix.

3.4.5.2. Discussion and modification of the experiment of microgel placement and plugging performance in commercial sand filled fracture. From the above experiment results, the gel placement performance was acceptable under the modification of this experiment.

The acceptable performance can be confirmed in following discussion. First, different from the cross-sectional view of previous experiment, regardless that the gel particle was produced or stopped injecting the gel particles before the pressure built up sharply, the repackage issue in sand filled area in this experiment had been eliminated by packing the sand tightly enough using tools. For instance, compared with the cross-sectional view in experiment MPA-1, there was not an obvious separation between the sand area and gel particle. Oppositely, the gel particle distributed in the sand area uniformly. Second, in the discussion of experiment MPA-2, the conclusion that choosing a smaller size of gel particles had a positive effect on gel placement performance had been found. This conclusion had been verified again in this experiment MPC-0. Compared with the cross-sectional view in experiment DE-2 and this experiment MPC-0, both of the gel particles were produced. However, the gel particles were injected into the whole channels between the sand grains in the experiment MPC-0 while cumulated as a mass and penetrated the sand filled area in experiment DE-2. In addition, the gel placement performance in experiment MPC-0 is similar to that in experiment DE-2. Thus, it was proved again that smaller size had a positive effect on gel placement performance. Third, by comparing with the lateral view results in previous experiments, a fragmentary gel cake was found in experiment MPC-0. The gel particles mainly accumulated at the inlet of sand filled area instead of the matrix side surface. The formation of the fragmentary gel cakes, instead of dense and intact ones that observed in previous experiments, is an excellent result after gel injection as analyzed in result part which matched the conclusion in SPE - 89468- PA that the softer gel particle can pass the channel easier due to the tendency to deform.

Modification for next experiment. According to the discussion above, the results of gel placement performance were admissible. However, the evaluation of gel plugging performance was not provided because an integrated core flooding process hadn't been done. Therefore, considering the results and observation in previous experiments, the following modifications will be proceeded for next experiments:

1. Experimental materials modification. Since 170-230 mesh size gel was successful to inject into model of experimental MPA-2, the next two experiments will be processed with different mesh size of gel, which were 170-230 mesh size and below 230 mesh size. After finishing two experiments, the experimental results and the influences between two different sizes gel will be analyzed and compared.

2. The experimental objective modification. To finish the objective, after saturating the oil in the experimental models and processing two integrated core flooding experiments, the pressure behaviors will be analyzed and evaluated in detail.

3. The experimental procedure modification. Because there was no obvious change for the previous oil recover ratio curves in secondary water flooding process, thus in next experiment the core flooding process after gel injection should focus on polymer flooding instead of low salinity water flooding, which needs stop injecting polymer solution when water cut reach nearly 100%.

3.4.6. The Results of the Gel Treatment in Commercial Sand Filled Fracture. The below content covered the results and modification of the gel application in commercial sand filled fracture experiment after the modification of macroscopic experiment of gel application in Alaska sand filled fracture.

3.4.6.1. Experiment results of microgel placement and plugging performance in commercial sand filled fracture. *The results of water cut, oil recovery ratio, and pressure behavior in the experiment MPC-1.* In the last experiment, the evaluation of the gel plugging performance was not provided. Thus, to finish the objective of evaluating the gel plugging performance, two experiments were processed by following the modification mentioned in last experimental discussion part. The results of oil recovery ratio, water cut and pressure behavior were shown in Figure 3.31 and 3.32.

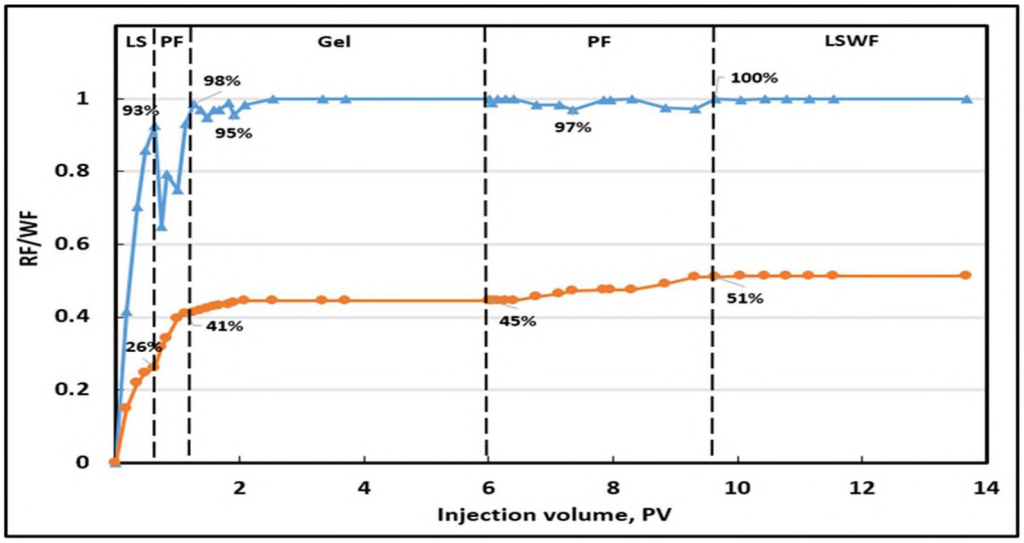

Figure 3.30 The results of water cut, oil recovery ratio in experiment MPC-1.

The results of water cut, oil recovery ratio, and pressure behavior in the experiment MPC-1. In experiment MPC-1, the gel particles selected to inject were below 230 mesh size. As shown in Figure 3.31, before the gel flooding process, the water cut and oil recovery ratio kept increasing in general. Tt the end of polymer injection, the RF

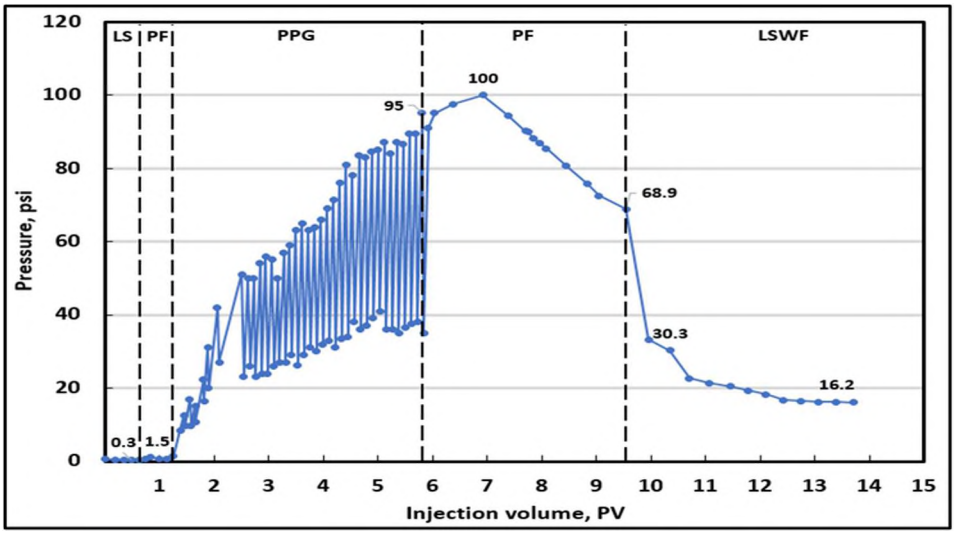

Figure 3.31 The results of pressure behavior in experiment MPC-1.

and FW increased to around 41% and 98%. However, the water cut decreased from 93% to around 65% when the polymer solution was injected to approximately 0.2 PV and the oil recovery ration increased to 33% from 26% correspondingly. This descent was due to the higher macroscopic displacement efficiency caused by the more viscous displacing fluid. Then during the gel flooding process, the total volume of gel particle injection was 4.6 PV. As shown in Figure 3.31, the oil recovery ratio increased to around 44% during the first 0.5 PV gel particle injection and then kept constant until stopped injection. However, different from the insignificant change for the oil recovery ratio curve, the pressure in Figure 3.32 behaved as an up trending zigzag curve and performed significant fluctuations through the whole gel flooding process. During the process of these fluctuations in gel flooding, there was no gel particle produced but some oil was produced before the pressure reached 50 psi when the fluctuations were not frequent. However, no more oil was produced when the pressure reached around 50 psi but the gel particle was produced for the first time. Then at the same time, the first large pressure

descent happened that the pressure decreased from 50 psi to 23 psi. After the first-time gel particle production, the gel was kept being produced during following pressure fluctuations. The peak pressure value of each new fluctuation was mostly higher than the previous one. However, it was very difficult to record how much gel had been produced under each fluctuation due to too many frequent fluctuations. When the pressure increased to around 95 psi, the second polymer flooding was conducted. The pressure kept increasing to around 100 psi after first 0.7 PV polymer solution injection and there was no oil and gel particle produced during this increment. Thus, the water cut and the oil recovery ratio kept constant. However, when the pressure reached approximately 100 psi, the pressure breakthrough happened, both oil and gel particles began to produce from the outlet. The producing processes of oil and gel particle were continued until the pressure decreased to nearly 69 psi. Although the oil recovery ratio increased from 45% to 51% during the whole polymer flooding, it was not satisfactory because the gel particle was also been produced simultaneously by polymer solution which indicated the polymer impaired the gel plugging efficiency. However, due to purple dye influence, it's difficult to estimate how much of the gel particle was produced during the polymer flooding process. At the end of the polymer flooding process, the water cut reached nearly 100% with no more oil and gel particles being produced, and the pressure decreased to 51psi correspondingly. For the final low salinity water flooding, the pressure kept decreasing to 30 psi and remained stable at 16 psi during final 2 PV water injection with no more oil and gel particle being produced because the displacing channel had been formed during the polymer flooding and no more remaining oil was left in this channel.

The results of water cut, oil recovery ratio, and pressure behavior in the experiment MPC-2. In experiment MPC-2, the gel particles selected to inject were 170-230 mesh size and the oil recovery ratio, water cut and pressure behavior were shown in Figure 3.33 and 3.34.

As shown in Figure 3.33, the water cut and oil recovery ratio kept increasing in general before the gel flooding process. At the end of the polymer injection, RF and FW increased to around 42% and 98%. The water cut decreased from 93% to around 62% when the polymer solution was injected to approximately 0.25 PV and the oil recovery ration increase to 38% from 30 correspondingly. This descent was also caused by improving the macroscopic displacement efficiency using more viscous displacing fluid. Then during the gel flooding process, the total injection volume of gel particle was 4.5 PV. As shown in Figure 3.33, the oil recovery ratio increased to around 46% during the

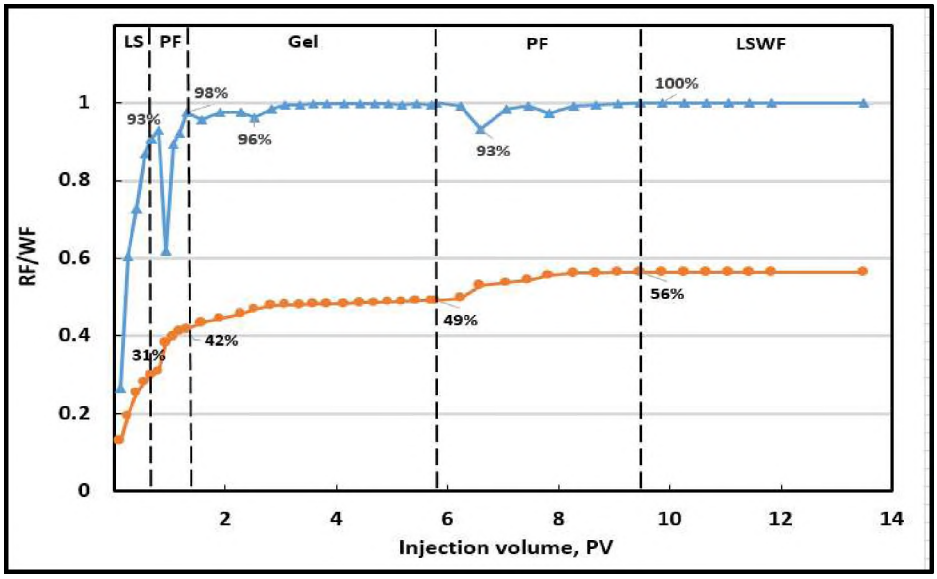

Figure 3.32 The results of water cut and oil recovery ratio in experiment MPC-2.

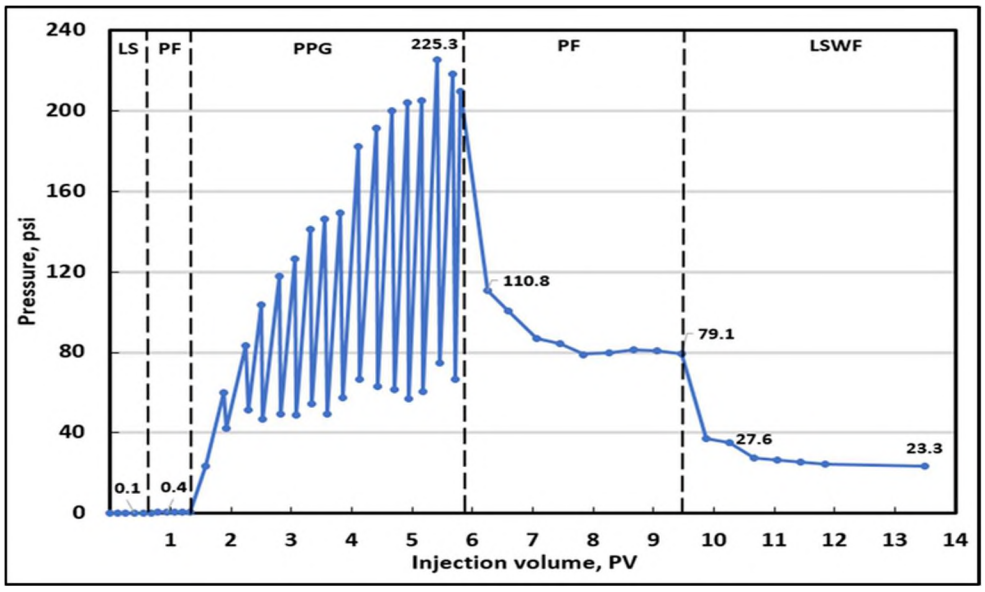

Figure 3.33 The results of pressure behavior in experiment MPC-2.

first 0.9 PV gel particle injection and then kept constant until the injection was stopped. Similarly, to MPC-1. Regardless of the insignificant change in the oil recovery ratio curve, the pressure curve shown in Figure 3.34 also behaved as an up trending zigzag shape and performed significant fluctuations throughout the whole gel flooding process. During the process of these fluctuations in gel flooding, there was also no gel particle produced but only some oil was produced. The fluctuations were not frequent before the pressure reached 115 psi. Yet when the pressure reached around 115 psi, no more oil was been produced but the gel particle began to produce for the first time with the first-time pressure descent from 115 psi to 49 psi. Sequentially after the first-time gel particle was produced, the rest of the gel was kept being produced during following pressure fluctuations with the new peak pressure value of each fluctuation was higher than the previous one. However, due to the frequent fluctuations, it was still hard to record how much gel had been produced under each fluctuation. When the pressure increased to

around 220 psi, the second polymer flooding was processed. Different from MPC-1, the pressure breakthrough directly happened at the beginning of the polymer flooding process as the pressure decreased to around 110 psi during first 0.44 PV polymer solution injection and both oil and gel particles began to produce from the outlet. The producing processes of oil and gel particle were continued until the pressure decreased to nearly 79 psi. Although the oil recovery ratio increased from 49% to 56% during the whole polymer flooding process, it was still not satisfactory because that the gel particle was produced by polymer solution again which indicated the polymer for the second time impaired the gel plugging efficiency. However, due to purple dye influence, it's difficult to estimate how much of the gel particle was produced during the polymer flooding process. At the end of the polymer flooding process, the water cut reached nearly 100% and no more oil and gel particles were produced with the pressure decreased to 79 psi correspondingly. For the final low salinity water flooding, the pressure kept decreasing to 35 psi and remained stable at 23 psi during final 2 PV water injection. No more oil and gel particle were produced during the final water flooding process, because no more remaining oil left in this channel formed and displaced during last polymer flooding.

The results of gel migration in lateral view and the cross-sectional view of the experimental model.MPC-1 Based on the results of the cross-sectional view of experiment models in Figure 3.34 and 3.35, although different mesh size gel particles were injected into two experimental models, they were both injected into the channels between the sand grains. Comparing two cross-sectional views in Figure 3.34 and 3.35, the distribution of smaller size gel in Figure 3.34 was more uniform than that in Figure 3.35 as the gel particle distribution was reduced gradually from the left inlet to right inlet.

This distribution difference was caused by more frequent pressure fluctuations happened in smaller size gel injection. In another word, under the same gel volume injection, smaller size gel particles had more opportunities to be placed into the channels between san grains. Thus, the pore volume occupied by smaller gel particles was larger than that occupied by bigger size gel particles in two experimental model with same dimensions.

Figure 3.34 The cross-sectional view of experiment model with injecting below 230 mesh size gel.

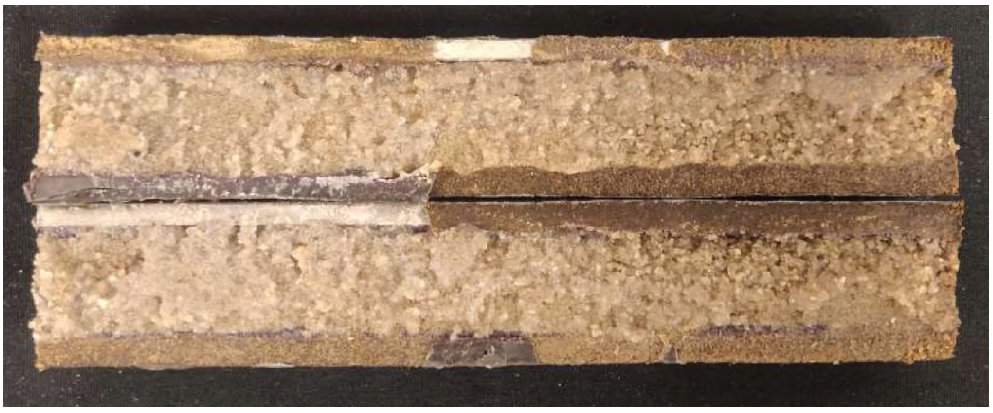

Figure 3.35 The cross-sectional view of experiment model with injecting 170-230 mesh size gel.

For the lateral views of both experimental models in Figure 3.36 and 3.37. Two lateral views illustrated two fragmentary and penetrable gel cakes were formed. The gel particles on two gel cakes both mainly concentrated on the middle inlet of filled sand area which was caused by the softer gel property that is willing to deform and go through the channel. The gel particles remained on the matrix side surface were penetrable for both of the models. Some areas of the matrix were not covered by the gel particles because they were penetrated by the polymer solution and in turn diverted the polymer into the matrix at a lower pressure. However, the gel cake formed by smaller size gel particles performed a less dense property than the ones formed by larger size gel particles. This was due to the dehydration property of the gel that larger size gel particles tend to dehydrate more water than the smaller size gel particles under the same pressure.

Figure 3.36 The lateral view of experiment model with injecting below 230 mesh size gel.

3.4.6.2. Discussion and modification of the experiment of microgel placement and plugging performance in commercial sand filled fracture. *Discussion of MPC-1 and MPC-2.* According to the results above, three main sections of results will be discussed in terms of comparing MPC-1 and MPC-2 with previous experiments results, the discussion of zigzag pressure curve, and comparing the results of MPC-1 and MPC-2 alone.

Figure 3.37 The lateral view of experiment model with injecting 170-230 mesh size gel.

Overall, comparing the MPC results to previous results, the results in experiment MPC were more acceptable than those in all previous results. Specifically, the main experiment of comparison is experiment DE-2 because the MPC experiments were processed under similar experiment procedures as those in DE experiments and the gel particles were both produced out from the outlet. First of all, before the gel flooding process, the larger sand grains generated high permeability zones where the larger channels were created and more oil was saturated. As a result, after first water and

polymer solution flooding processes, the oil recovery performance was more prominently as the water cut decreased more obviously, 65% in MPC-2 compared with 75% in DE-2. Besides, the oil recovery ratio at the end of polymer flooding was also higher with 40% in MPC-2 than 29% in DE-2. Second, during the gel flooding process, although the oil recovery ratio in two experiments both increased, the oil was displaced during gel flooding is not a good prospection because the effect of gel particles in such scenario is as the displacing agent instead of plugging agent. However, the mechanisms of displacement processes in two experiments were different. The mechanism in previous experiment DE-2 was repacking the filled sand and squeezing the oil come out but in experiment MPC-2 was the gel particles displaced the oil in channels between sand grains. Moreover, because the gel in experiment MPC-2 is a kind of higher swelling ratio gel particle and pressure fluctuations frequently happened, thus at the same time of gel particles migration in the channels, some brine solution was dehydrated from the gel particles and diverted to the matrix to displace some oil saturated within. By contrast, the pressure in experiment DE-2 just directly built up more than 1000 psi, and the gel particles cumulated as a mass and penetrated the sand area with no more gel particles were placed in the channels between the sand grains and less brine dehydrated from the gel particles diverted into matrix. Finally, compared the results after gel flooding between the experiment MPC-1 and DE-2, although the increment of oil recovery ratios in two experiment were nearly same as around 6%, the breakthrough pressures were significantly different with 100 psi in MPC-2 compared with 1230 psi in DE-2. Besides, the oil and gel were both produced in MPC-1 but only gel was produced in DE-2. For the huge differences between breakthrough pressures, the main reason is the gel cake effect.

As shown in Figure 3.17, a denser and intact gel cake was formed in experiment DE-2 while a fragmentary and penetrable gel cake was formed in experiment MPC-2 in Figure 3.37. The much denser gel cake required a higher pressure to breakthrough, thus, an obvious pressure difference occurred. After polymer solution broke through the gel cake due to the higher viscosity of polymer than gel, some gel particles were produced by the polymer solution that being injected into the middle sand filled area. Based on the cross-sectional views in two experiments and the above-mentioned discussion of gel flooding process, the gel particles in experiment DE-2 did not played an effective role in plugging channels and reducing the permeability. In contrast, the gel particles in experiment MPC-2 distributed uniformly in the channels between the sand grains and thus played a significant role in respect of plugging the channels and reducing the permeability. As a result, some polymer solution diverted into the matrix and displaced the oil in the matrix, due to the gel plugging effect.

Zigzag pressure behavior in experiments MPC. Different from the pressure behavior in experiment DE-2 that the pressure directly built up to 1000 psi because the gel cake blocked the later gel particle injection, the pressure behavior in experiments MPC behaved as a frequent fluctuation curve with a zigzag shape as shown in Figure 3.32 and 3.34. Generally, the zigzag pressure behavior represents the gel particles being repeatedly entered and re-entered the pore spaces between the sand grains during the gel injection. The Figure 3.38 illustrated the zigzag curve behavior in detail. As shown in Figure 3.38, the experimental model was sketched and separated into three parts which is consider as integral methods. The background fracture, gel particles and sand grains were in purple, tawny and brown, respectively. First, before the gel particles were injected into

the spaces between the sand grains and the injection pressure increases gradually as shown in the Figure 3.32 and 3.34 which indicated the pressure build-up process that the potential energy being storage. Then a breakout pressure met and the pressure decreased rapidly. Simultaneously, the gel particles were injected into the first area of Figure 3.39 (B), which caused the descent of pressure that the potential energy being released as illustrated in the sketch of Figure 3.39 (B). Then the gel particles will repeat the same two procedures: first stuck to accumulate the potential energy and then broke through to release the potential energy. However, since the gel particles have already occupied in first area of middle sand filled area, the resistance was increased so that the breakout pressure needed for next gel injection would be higher, and it would gradually increase after each 'energy storage and release' process to form an up trending zigzag pressure curve.

The differences of MPC-1&2 is mainly forcing on gel flooding process and polymer flooding process.

Gel flooding:

1. RF increment difference: 4%@ 230 mesh size to 7%@170-230 mesh size.

2. Pressure fluctuation difference: The peak pressure difference 100 psi vs 225.3 psi. It means the plugging efficiency is better for a large size gel than a small size one. In other word, higher pressure indicates the permeability difference is smaller between matrix and sand area, thus more dehydrate or carried water divert to matrix, as a result, more oil was displaced.

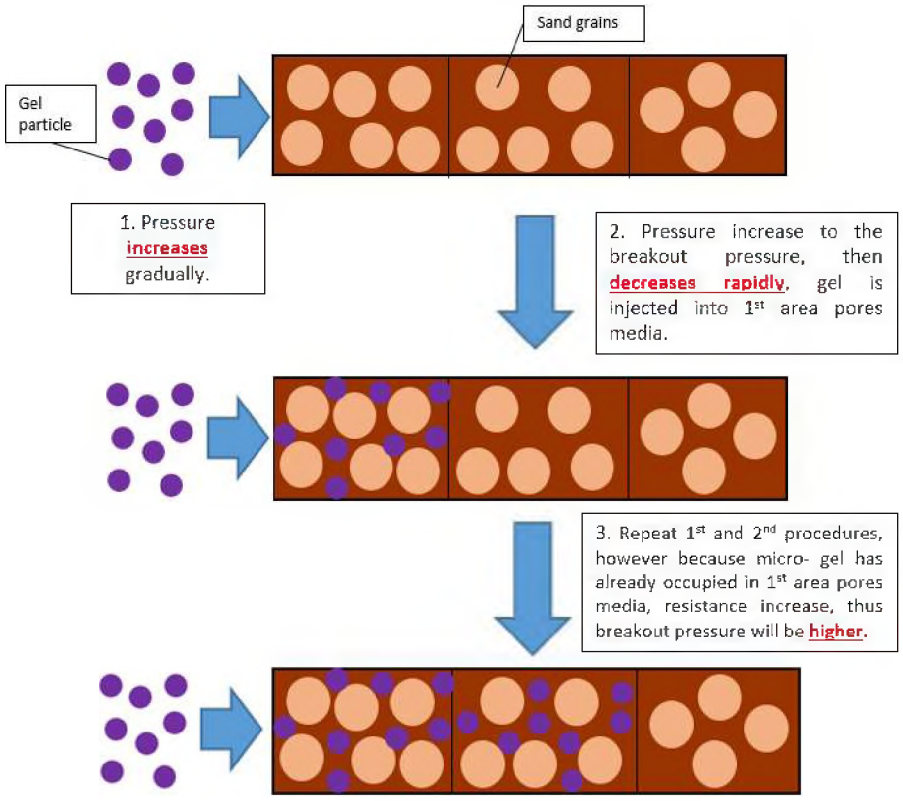

Figure 3.38 The process of gel particle injection.

Thus, pressure fluctuation reflected the RF increment difference.

Polymer flooding:

1. There was no significant difference in terms of increment of RF curves. However, the variations were apparently different. For the 230 mesh size sands, it showed a stair-stepping type to continuously rise while for 170-230 mesh sands it showed a steep incremental in first 0.6PV injection and then the tendency to steady.

2. The decreases of FW curves were significantly different. For the 230 mesh size sands, the water cut fluctuated between 97% to 99% during PF. For 170-230 mesh size sands, it directly decreased to 93% and then increased to nearly constant 99%.

3. The pressures to start injecting polymer solution were different. The pressure for 230 mesh size sands first increased to 100 psi transitorily then consistently decreased, this pressure increment was because the starting injection polymer solution pressure is at a lower level, 37psi, thus, the pressure needed to build up to breakthrough. However, for 170-230 mesh size sands, it decreased to 110.8 psi in first 0.6 PV and trended to constant gradually, this pressure descent was because the starting injection polymer solution pressure is at a higher level, 210psi, thus, the pressure breakthrough happened directly.

Moreover, the reason why the whole pressure behaviors in two experiments were significantly different, it was because of the different plugging performance that the larger size gel has a better plugging performance than the smaller size gel. Besides, the polymer resistances to gel particles were different. Thus, the situations of gel particle produced during polymer flooding were different. The gel particles were continually produced out during the later polymer and water flooding in smaller size gel application experiment, however, the volume of produced gel particles decreased gradually until no more gel particles were produced out during the later polymer and water flooding in larger size gel application experiment.

To sum up, selecting larger size gel particle was better than the smaller size gel. No matter the displacement performance in gel flooding or the gel plugging performance in second polymer flooding.

3.5. DISCUSSION

For the discussion in the section 3.3, it mainly discussed the relationship between 'before and after' experimental groups. For the discussion in this section, by comparing and referring to the conclusions of the literatures in previous literature review part, the microgel plugging and placement performance in sand filled fracture were discussed.

PPG injection Pressure behavior. As a whole, the pressure trend in the study of this thesis and the study of PPG application in super-K sand pack which was finished by Imqam et al are similar that the injection pressure increases gradually and finally reached plateau. However, even the trend behavior is semblable, the pressure variations in the trend are obviously different. Both pressure fluctuations happened in two papers, but the amplitudes were significantly different. A high- amplitude pressure behavior was illustrated in sand filled fracture, and in contrast, the low- amplitude fluctuations accompanied all pressure trend in sand pack experiment. The crucial reason why different amplitude fluctuations happened in two experiments was the heterogeneity difference. Although Imqam et al (Imqam et al., 2015) filled the commercial silica sand in the sand filled tube model to create the sand pack and finish the experiment, it is obviously less heterogeneous than the sand-filling fractured model. Selecting the sandstone with the permeability of 500 md as the matrix to create the fracture and filling the silica sand with the permeability of 1000 to 3000 md to finish the model construction will lead to an obvious heterogeneity difference than that of the sandpack with the same sizes of sands. Combining the Figure 3.39 and the heterogeneity difference can explain why the pressure fluctuation amplitudes are different. As shown in Figure 3.39, the gel particle can be injected into the space between sand grains uniformly as a whole. However, due to the

heterogeneity difference, the homogeneous gel migration scenario in the spaces between sand grains will not appear in the sand-filling fractured model. Instead, the gel particles will be cumulated as a gel cake on the surface of the experimental model at first, then the later gel particle will break through the gel cake which is at the inlet of the side surface of sand filled area when the pressure reaches a specific level. After breakthrough, the gel particles will be injected into the spaces between the sand grains, and meanwhile, some gel cake will still remain on the injection area and accumulate as the gel cake again. Since some gel particles have already been injected into the spaces between the sand grains and develop the effect of the plugging performance, the later breakthrough pressure should be higher than before.

To sum up, the heterogeneity difference is caused by experimental model construction and the directly reason to induce the gel cake cumulation during gel flooding process, which leads to a high- amplitude fluctuation happened in pressure curves.

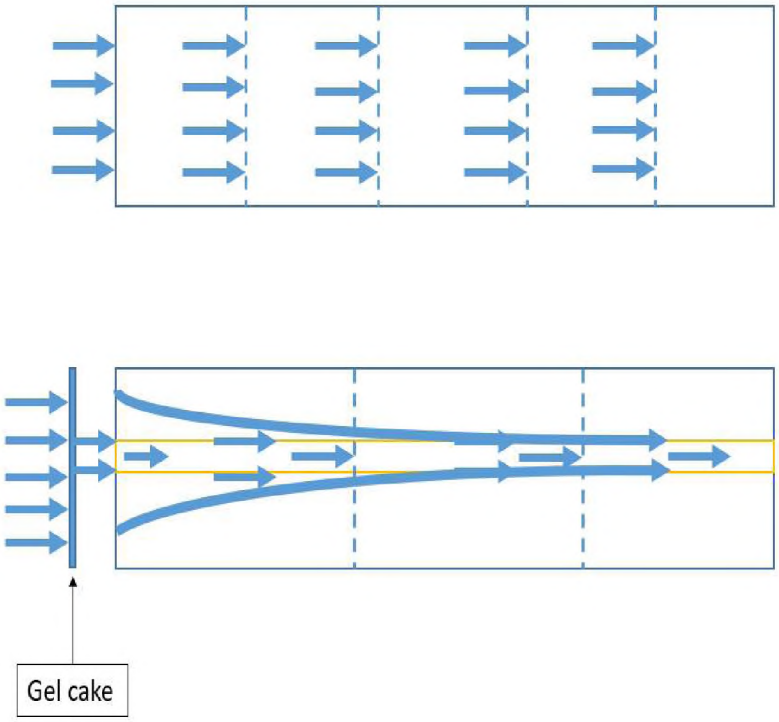

Figure 3.39 The sketches of gel transport mechanism in sand pack and sand filled fracture.

4. CONCLUSIONS AND RECOMMENDATIONS

4.1. CONCLUSIONS

In this study, several factors have been investigated regarding microgel treatment for improving the conformance control of polymer flooding in heavy oil using heterogenous models with sand-filling fractures. The following conclusions can be drawn from this research:

- Adopting Epoxy to seal the sand filled fracture model and using tools to compact the sand filled fracture are essential to avoid non-ideal gel propagation and sand repackage issue.
- When injecting the microgel into a heterogeneous fractured channeling model, a gel cake is formed on the inlet surface of matrix which could damage the matrix and result in the obvious pressure increase during following displacing fluid injection.
- Without considering the chemical methods to remove the gel cake, less PPG injection volume, smaller size PPG injection and higher swelling ratio PPG injection can mitigate the influence of the gel cake on blocking the matrix.
- Comparisons between gels with different swelling ratios, the higher swelling ratio gel particle has a positive effect in terms of gel propagation and plugging performance in the channel and oil recovery improvement in our models.
- Microgel with a higher swelling ratio preforms a continued up-trending zigzag pressure curve during the gel particle injection process in the sand-

filling fracture and gradually reached to a plateau. The range, frequency and the peak of the pressure fluctuation were different when selecting different microgel sizes.

- Microgel with a higher swelling ratio could propagate deeply into the fluid channel. However, it was observed that the different sizes microgel were displaced out during followed polymer or water injection processes, which can cause an impairment to the plugging efficiency. However, this issue can be mitigated by selecting a larger size gel.
- The smaller size gel has a better performance than larger size gel when injecting the gel particle with a lower swelling ratio, in terms of the gel placement, plugging efficiency in the sand-filling fracture for a higher oil recovery ratio.

4.2. RECOMMENDATIONS

In the whole work, because the polymer impairment issue has not been completely overcome, we recommend to use the microgel with re-crosslinked properties instead of normal preformed particle gel to proceed the further experiments.

BIBLIOGRAPHY

Al-Assi, A. A., Willhite, P. G., Don, G. W. and McCool, S. C., Formation and Propagation of Gel Aggregates Using Partially Hydrolpzed Polyacrylamide and Aluminum Citrate, SPE-100049-MS (2006).

Abdulmohsin Imqam, Ze Wang, Baojun Bai., The plugging performance of preformed particle gel to water flow through large opening void space conduits, Journal of Petroleum Science and Engineering,Vol 156, PP. 51-6 (2017).

Alhuraishawy, A. K., Bai, B., Wei, M., Almansour, A., Alsaba, M., & Elsharafi, M. Integrating Microgel-Low Salinity Waterflooding to Improve Production Profile in Non-Crossflow Heterogeneous Reservoir. Society of Petroleum Engineers. doi:10.2118/192154-MS (2018, August 16).

A Zaitoun, R Tabary, D Rousseau, et al. Using microgels to shut off water in a gas storage well, International Symposium on Oilfield Chemistry, Houston (2007)

Bai, B. and Zhou, J., Yin, M., A Comprehensive Review of Polyacrylamide Polymer Gels for Conformance Control., Petroleum Exploration and Development, doi:10.1016/S1876-3804(15)30045-8 (2015).

Bai, B., Huang, F., Liu, Y., Seright, R. S., & Wang, Y., Case Study on Prefromed Particle Gel for In-Depth Fluid Diversion. Society of Petroleum Engineers. doi:10.2118/113997-MS (2008).

Bai, B., Liu, Y., Coste, J.-P. and Li, L., Preformed Particle Gel for Conformance Control: Transport Mechanism Through Porous Media, SPE-89468-PA (2007).

Bai, B., Li, L., Liu, Y., Liu, H., Wang, Z. and You, C., Preformed Particle Gel for Conformance Control: Factors Affecting Its Properties and Applications, SPE-89389-PA (2007).

Bai, B., Wei, M., Liu, Y., Field and Lab Experience with a Successful Preformed Particle Gel Conformance Control Technology, SPE-164511-MS (2013).

Chang P W, Gruetzmacher G D, Meltz C N, et al. Enhanced hydrocarbon recovery by permeability modification with phenolic gels: US, 4708974A. 1984-10-01.

Chauveteau, G., Omari, A., Tabary, R. et al., New Size-Controlled Microgels for Oil Production, SPE-64988-MS (2001).

Chauveteau, G., Tabary, R., Bon, C. et al., In-Depth Permeability Control by Adsorption of Soft Size-Controlled Microgels, SPE-82228-MS (2003).

Chuan-jin, Y., et al., Study on Plugging Performance of Pore-scale Elastic Microspheres. Science Technology and Engineering, 2012(06): p. 1244-1247.

Coste, J. –P., Liu, Y., Bai, B. et al., In-Depth Fluid Diversion by Pregelled Particles, SPE-59362-MS (2000)

Dovan H T, Hutchins R D, Sandiford B B. Delaying gelation of aqueous polymers at elevated temperatures using novel organic crosslinkers. SPE 37246-MS, 1997.

D W Green, G P Willhite Improving reservoir conformance using gelled polymer systems, Univ. Lawrence, Kansas (1995)

Ecological Analysts Inc The sources, chemistry, fate, and effects of chromium in aquatic environments, American Petroleum Institute, Washington D C (1981)

Elsharafi, M. O., & Bai, B. (2013, June 10). Effect of Strong Preformed Particle Gel on Unswept Oil Zones/Areas during Conformance Control Treatments. Society of Petroleum Engineers. doi:10.2118/164879-MS

Fakher, Sherif & Bai, Baojun & Imqam, Abdulmohsin & Wang, Yanling.. Novel Mathematical Models to predict Preformed Particle Gel Placement and Propagation through Fractures. 10.2118/187152-MS (2017).

Frampton H, Morgan J C, Cheung S K, et al. Development of a novel waterflood conformance control system. SPE 89391-MS, 2004.

F S Seright, F D Martin Fluid diversion and sweep improvement with chemical gels in oil recovery processes, Petroleum Research Center, New Mexico (1991)

Goudarzi, A., et al., New Experiments and Models for Conformance Control Microgels. 2014, Society of Petroleum Engineers.

Hutchins R D, Dovan H T, Sandiford B B. Field applications of high temperature organic gels for water control. SPE 35444-MS, 1996.

Imqam, A., Bai, B., Al-Ramadan, M. et al., Preformed Particle Gel Extrusion through Open Conduits during Conformance Control Treatments, SPE-169107-PA (2015).

Imqam, A., B. Bai, and M. Wei, Combining Conformance Treatment with Mobility Control Improves Oil Sweep Efficiency in Non-Cross Flow Heterogeneous Reservoirs. 2015, Society of Petroleum Engineers.

Imqam, A., Bai, B., Elue, H. and Muhammed, F., Use of Hydrochloric Acid to Remove Filter Cake Damage from Preformed Particle Gel during Conformance Control Treatments, SPE-172352-PA (2016).

Imqam, A., Bai, B., Xiong, C., Wei, M., Delshad, M., Sepehrnoori, K., Characterizations of Disproportionate Permeability Reduction of Particle Gels through Fractures, SPE-171531-MS (2014).

Imqam, A., Elue, H., Muhammed, F. A., & Bai, B. Hydrochloric Acid Applications to Improve Particle Gel Conformance Control Treatment. Society of Petroleum Engineers. doi:10.2118/172352-MS (2014).

Imqam, A., Wang, Z., & Bai, B., Preformed-Particle-Gel Transport Through Heterogeneous Void-Space Conduits. Society of Petroleum Engineers. doi:10.2118/179705-PA (2017)

Liu, Y., Bai, B. and Shuler, P. J., Application and Development of Chemical-Based Conformance Control Treatments in China Oil Fields, SPE 99641 (2006).

Lin Sun, Qi Han, Daibo Li, Xiao Zhang, Wanfen Pu, Ximing Tang, Yongchang Zhang, and Baojun Bai., Water Plugging Performance of Preformed Particle Gel in Partially Filled Fractures. Industrial & Engineering Chemistry Research, 58 (16), 6778-6784 (2019).

Mack J C, Smith J E. In-depth colloidal dispersion gels improve oil recovery efficiency. SPE 27780-MS, 1994.

Majid Abedi Lenji, Masoud Haghshenasfard, Mohsen Vafaie Sefti., Mahsa Baghban Salehi, Aghdas heidari, Experimental study of swelling and rheological behavior of preformed particle gel used in water shutoff treatment, Journal of Petroleum Science and Engineering, 169: 739-747 (2018).

M. O. Elsharafi and B. Bai, "Effect of Weak Preformed Particle Gel on Unswept Oil Zones/Areas during Conformance Control Treatments," Industrial and Engineering Chemistry Research, vol. 51, no. 35, pp. 11547-11554, American Chemical Society (ACS), Sep 2012.

Morgan J C, Smith P L, Stevens D G. Chemical adaptation and development strategies for water and gas shut-off gel systems. Ambleside: 6th International Symposium, 1997.

Muhammed, Farag Awadh, "Study and pilot test on a novel EOR method - coupling PPG conformance control and surfactant flooding" Doctoral Dissertations. 2350 (2014).

Needham, R. B., Threlkeld, C. B. and Gall, J. W., Control of Water Mobility Using Polymers and Multivalent Cations, SPE-4747-MS (1974)

Pritchett J, Frampton H, Brinkman J. Field application of a new in-depth waterflood conformance improvement tool. SPE 84897, 2003.

Rousseau, D., Chauveteau, G., Renard, M., Tabary, R. and Zaitoun, A., Mallo, P., Braun, O., Omari, A., SPE 93254 (2005).

Seright Aperture-tolerant, chemical-based methods to reduce channeling, OSTI, Washington D C (2007)

Sydansk R D. A new conformance-improvement-treatment chromium (III) gel technology. SPE 17329-MS, 1988.

Southwell G P, Posey S M. Applications and results of acrylamide-polymer/chromium (III) carboxylate gels. SPE 27779-MS, 1994.

Xindi Sun, Ali K. Alhuraishawy, Baojun Bai, Mingzhen Wei., Combining preformed particle gel and low salinity waterflooding to improve conformance control in fractured reservoirs, Fuel Journal, 221: 501-512 (2018).

Y Zhuang, S N Pandey, C S McCool, et al.Permeability modification with sulfomethylated resorcinol-formaldehyde gel system SPE Reservoir Evaluation & Engineering, 3 (5) (2000), pp. 386-393

Zhang, H., Bai, B., Preformed Particle Gel Transport through Open Fractures and its Effect on Water Flow, SPE 129908 (2010).

Zhaojie Song, Baojun Bai, Hao Zhang., Preformed particle gel propagation and dehydration through semi-transparent fractures and their effect on water flow, Journal of Petroleum Science and Engineering, 167: 549-558 (2018).

VITA

Baihua Lin received his Bachelor of Science degree in Petroleum Engineering from Missouri University of Science and Technology in May 2018. He began pursuing his master's degree in Petroleum Engineering at Missouri University of Science and Technology in August 2018. In May 2020, he received his Master of Science in Petroleum Engineering from Missouri University of Science and Technology.